

# POLITECNICO DI TORINO

Master of Science in Biomedical Engineering

Master Thesis

*Establishing the rationale for the design of an enhanced  
mRNA vaccine based on hybrid nanosystems:  
use of lipid-coated nanoparticles*



## **Advisor**

Prof. Valentina Alice Cauda  
Prof. Salvador Borrós Gómez  
Dr. Cristina Fornaguera Puigvert

## **Candidate**

Gae Azzara

March 2021

*A mio Papà*



## RINGRAZIAMENTI

Arrivata alla fine della mia tesi e della mia carriera universitaria, vorrei dedicare questo spazio a tutti coloro che sono stati indispensabili per la realizzazione di questo lavoro.

Innanzitutto, vorrei ringraziare la mia relatrice Valentina Cauda, grazie per avermi scelto per questo progetto, per aver creduto in me e nelle mie potenzialità ma soprattutto nelle mie forti motivazioni, nonostante provenissi da un corso di laurea leggermente diverso da quello a cui lei era abituata.

Grazie al Prof. Salvador Borrós e alla Dott.ssa Cristina Fornaguera per avermi accolto nel vostro team e seguito durante il mio progetto a Barcellona. Un enorme grazie a tutto il gruppo GEMAT, al team di Tractivus, ai dottorandi e alle mie colleghe tesiste e amiche Laura, Monica e Gloria. Tornerò presto a salutarvi.

Alle mie amiche Clara, Adriana e Nadia, mi avete sostenuto nei momenti difficili, quando eravamo vicine ma ancora di più quando ero lontana. Mi avete accolto in casa vostra quando avevo bisogno di solitudine, mi avete sopportato e supportato e avete sempre saputo consigliarmi saggiamente. Per tutto questo vi ringrazio.

Un enorme grazie alle mie amiche Carla e Francesca con le quali ho condiviso gran parte dei miei anni accademici, esami, pranzi, cene, viaggi. La nostra amicizia continuerà, senza ombra di dubbio, oltre le mura del Politecnico.

Grazie a tutti i miei amici d'infanzia, soprattutto a Francesco che ha condiviso con me gli ultimi mesi di studio folle e disperato, tra pause cibo e pause corsa.

Grazie ad Amelia, coinquilina, amica, confidente, compagna di mille avventure, *soul sister*. Con te ho condiviso 8 anni della mia vita in simbiosi, lacrime, sofferenza ma soprattutto momenti felici. La nostra amicizia durerà per sempre. Grazie anche a Merlino e Woody, l'amore per gli animali va oltre ogni confine.

Grazie alla mia splendida famiglia, mia madre Rosa, Alain, Agata, Luca e le mie meravigliose nonne. Senza di voi questi mesi di quarantena sarebbero stati molto noiosi.

Infine, il più grande ringraziamento va a mio padre Nicolò, la persona più importante della mia vita, il mio esempio da seguire, fonte inesauribile di valori e conoscenze. Grazie per avermi trasmesso la passione e la serietà per questa professione, la curiosità per il mondo e scusa se a volte ti ho deluso. Questa tesi è dedicata a te.

*Gae*

## **ACKNOWLEDGMENTS**

Having reached the end of my thesis and my university career, I would like to dedicate this space to all those who have been indispensable for the realization of this work.

First of all, I would like to thank my supervisor Valentina Cauda; thank you for having chosen me for this project, for having believed in me and in my potential but above all in my strong motivations, despite the fact that I came from a degree course slightly different from the one you were used to.

Thanks to Prof. Salvador Borrós and Dr. Cristina Fornaguera for welcoming me into your team and following me during my project in Barcelona. A big thank you to the whole GEMAT group, to the Tractivus team, PhD students and my fellows and friends Laura, Monica and Gloria. I will be back soon to say hello.

To my friends Clara, Adriana and Nadia, you supported me during hard times, when we were close but even more when I was far away. You welcomed me in your home when I needed solitude, you have put up with me and have been able to advise me wisely. For all of this I thank you.

A huge thank you to my friends Carla and Francesca with whom I shared most of my academic years, exams, lunches, dinners, trips. Our friendship will continue, without a doubt, beyond the walls of the Politecnico.

Thanks to all my childhood friends, especially Francesco who shared with me last months of crazy and desperate studying, between food and running breaks.

Thanks to Amelia, flat mate, friend, confidante, partner of thousand adventures, soul sister. With you I shared 8 years of my life in symbiosis, tears, suffering but above all happy moments. Our friendship will last forever. Thanks also to Merlino e Woody, love for animals goes beyond all boundaries.

Thanks to my special family, my mother Rosa, Alain, Agata, Luca and my wonderful grandmothers. Without you months of quarantine would have been very boring.

Finally, the biggest thank you goes to my father Nicolò, the most important person in my life, my example to follow, inexhaustible source of values and knowledge. Thank you for giving me the passion and seriousness for this profession, curiosity about the world and sorry if sometimes I have disappointed you. This thesis is dedicated to you.

*Gae*

## ABSTRACT

According to the World Health Organization, cancer is a large group of chronic, difficult-to-treat diseases with more than ten million new cases each year, and it still remains the second leading cause of death in the world. In addition to mortality, it is also a significant cause of morbidity, due to the problems caused by traditional treatments, such as surgery, radiotherapy, chemotherapy or a combination of them. In recent years, research is strongly focused on finding new therapies that are effective and mostly with a lower incidence of side effects, among the latter, cancer immunotherapy is gaining attraction. Immunotherapies include various approaches among which **therapeutic vaccines** against cancer that are designed to boost the immune system to attack neoplastic cells via antigen presentation by dendritic cells. One of the major challenges of therapeutic vaccine concerns the design of an efficient vector for the *in vivo* delivery of antigens that allows transfection into specific immune cells. This project is the result of a collaboration between IQS of Barcelona and the Politecnico di Torino. The IQS group has previously demonstrated the remarkable versatile properties of end-modified poly ( $\beta$ -amino esters) oligopeptide (OM-PBAEs) to complex mRNAs and form discrete nanoparticles that enable specific targeting of antigen-presenting cells (APCs) *in vivo*. In contrast, at PoliTo, it was demonstrated how lipid nanosystems, composed of lipid-coated inorganic nanoparticles with antitumor properties, increase the cell penetration efficiency, biomimicry, non-immunogenicity, and bio-stability of inorganic nanoparticles. Combining both experiences, we focused on the development and study of non-viral vectors using liposome conjugated pBAE nanoparticles for an enhanced mRNA vaccine based on hybrid nanosystems. For this purpose, gold nanosystems have been first synthesized and characterized, in particular nanospheres and nanorods, which thanks to their inertness and stability allow to better perform the lipid coating following the solvent exchange method protocol. This method is based on the process of preparation of liposomes, called reverse-phase evaporation method, and with appropriate modifications allows to create a lipid membrane to the metal nanoparticles. Subsequently, two variants of the solvent exchange method have been tested on pBAE nanoparticles and characterization methods, such as NTA and CryoTEM, applied to demonstrate their encapsulation. Since the solvent exchange method is a process that uses, albeit in small amounts, ethanol, preliminary studies have been carried out to test the stability of the polyplexes in this solvent. However, considerable difficulties have been encountered with polymeric nanoparticles, which hardly maintained their stability during the encapsulation process and are therefore hardly visible in CryoTEM images. On the contrary, TEM images showed how gold nanosystems well interact with liposomes both internally and externally in small groups. However, the second encapsulation method for polymeric nanoparticles was chosen, which showed the synthesis of larger liposomes in which they

are expected to contain the nanoparticles. Subsequent steps of purification by sonication and filtration have been done to allow obtaining small size and monodisperse nanosystems and these results were also confirmed by fluorescent experiments in colocalization. Finally, preliminary *in vitro* transfection studies were performed on tumor cell line, chosen as a model, that showed an increase in transfection efficiency for liposome-conjugated nanosystems. Unfortunately, due to the Covid-19 situation some experiments were not possible to be carried out, including further studies on efficacy of cell transfection to confirm the validity of these results.

## RIASSUNTO

Secondo l'Organizzazione Mondiale della Sanità, il cancro è tra le più gravi malattie croniche e difficili da trattare, con più di dieci milioni di nuovi casi ogni anno, ed è la seconda causa di morte nel mondo. Oltre alla mortalità, è anche una causa significativa di morbilità, a causa dei problemi ed effetti collaterali derivati dai trattamenti tradizionali, come la chirurgia, la radioterapia, la chemioterapia o una loro combinazione. Negli ultimi anni, la ricerca è fortemente concentrata sulla ricerca di nuove terapie che siano efficaci e per lo più con una minore incidenza di effetti collaterali, tra queste ultime, l'immunoterapia sta guadagnando molta attenzione. Le immunoterapie includono vari approcci tra cui i **vaccini terapeutici** contro il cancro che sono progettati per stimolare il sistema immunitario ad attaccare le cellule neoplastiche attraverso la presentazione dell'antigene da parte delle cellule dendritiche. Una delle maggiori sfide dei vaccini terapeutici riguarda la progettazione di un vettore efficiente per il *delivery in vivo* di antigeni e che ne permetta la trasfezione in specifiche cellule immunitarie. Questo progetto è il risultato di una collaborazione tra l'IQS di Barcellona e il Politecnico di Torino. Il gruppo dell'IQS ha precedentemente dimostrato le notevoli proprietà versatili del poli( $\beta$ -amino esteri) oligopeptide-modificato (OM-PBAEs) per complessare l'mRNA e formare nanoparticelle discrete che permettono il targeting specifico delle cellule presentanti l'antigene (APCs) *in vivo*. Al contrario, al Politecnico, è stato dimostrato come i nanosistemi lipidici, composti da nanoparticelle inorganiche con proprietà antitumorali rivestite da lipidi, aumentano l'efficienza di penetrazione cellulare, la biomimetica, la non-immunogenicità e la bio-stabilità delle nanoparticelle inorganiche. Combinando entrambe le esperienze, ci siamo concentrati sullo sviluppo e lo studio di vettori non virali utilizzando nanoparticelle di pBAE coniugate con liposomi per un vaccino mRNA basato su nanosistemi ibridi. A questo scopo, sono stati prima sintetizzati e caratterizzati dei nanosistemi d'oro, in particolare nanosfere e nanobarre, che grazie alla loro inerzia e stabilità permettono di eseguire meglio il rivestimento lipidico seguendo il protocollo del metodo dello scambio di solventi. Questo metodo si basa sul processo di preparazione dei liposomi, chiamato metodo di evaporazione in fase inversa, e con opportune

modifiche permette di creare una membrana lipidica alle nanoparticelle metalliche. Successivamente, due varianti del metodo di scambio di solvente sono state testate su nanoparticelle di pBAE e metodi di caratterizzazione, come NTA e CryoTEM, sono stati applicati per dimostrare il loro incapsulamento. Poiché il metodo dello scambio di solventi è un processo che utilizza, anche se in piccole quantità, l'etanolo, sono stati effettuati studi preliminari per testare la stabilità delle nanoparticelle di pBAE in questo solvente. Tuttavia, notevoli difficoltà sono state riscontrate con le nanoparticelle polimeriche, che difficilmente hanno mantenuto la loro stabilità durante il processo di incapsulamento e sono quindi poco visibili nelle immagini CryoTEM. Al contrario, le immagini TEM hanno mostrato come i nanosistemi d'oro interagiscano bene con i liposomi sia internamente che esternamente in piccoli gruppi. Tuttavia, è stato scelto il secondo metodo di incapsulamento delle nanoparticelle polimeriche, che ha mostrato la sintesi di liposomi grandi e ben definiti in cui ci si aspetta contengano le nanoparticelle. Le fasi successive di purificazione con sonicazione e filtrazione sono state fatte per permettere di ottenere nanosistemi di piccole dimensioni e monodispersi e tali risultati sono stati confermati anche dagli esperimenti di co-localizzazione in fluorescenza. Infine, sono stati eseguiti studi preliminari di trasfezione *in vitro* su linee cellulari tumorali, scelte come modello, che hanno mostrato un aumento dell'efficienza di trasfezione per i nanosistemi coniugati con liposomi. Sfortunatamente, a causa della situazione Covid-19 non è stato possibile effettuare alcuni esperimenti, compresi ulteriori studi sull'efficacia della trasfezione cellulare per confermare la validità di quest'ultimi risultati.

# TABLE OF CONTENTS

<b>RINGRAZIAMENTI</b> .....	<b>I</b>
<b>ACKNOWLEDGMENTS</b> .....	<b>II</b>
<b>ABSTRACT</b> .....	<b>III</b>
<b>RIASSUNTO</b> .....	<b>IV</b>
<b>TABLE OF CONTENTS</b> .....	<b>VI</b>
<b>Chapter I. Motivations and Aims</b> .....	<b>1</b>
<b>1.1 Motivations</b> .....	<b>1</b>
<b>1.2 Aims</b> .....	<b>6</b>
<b>Chapter II. Background</b> .....	<b>7</b>
<b>2.1 Cancer Therapeutic Vaccines</b> .....	<b>8</b>
<b>2.2 Gene Transfer Methods</b> .....	<b>11</b>
2.2.1 Lipid Nanosystems .....	12
2.2.2 Polymeric Nanosystems.....	15
2.2.2.1 Poly ( $\beta$ -amino ester)s (pBAE).....	15
<b>2.3 Inorganic Nanoparticles in Cancer Treatment</b> .....	<b>17</b>
2.3.1 Gold Nanoparticles .....	18
2.3.2 Zinc-oxide Nanoparticles .....	19
2.3.3 Mesoporous-silica Nanoparticles .....	19
2.3.4 Superparamagnetic iron-oxide Nanoparticles (SPIONs).....	20
<b>2.4 Theranostic Systems</b> .....	<b>22</b>
<b>Chapter III. Materials and Methods</b> .....	<b>24</b>
<b>3.1 Materials</b> .....	<b>24</b>
<b>3.2 Synthesis of Nanosystems</b> .....	<b>24</b>
3.2.1 Liposomes .....	24
3.2.2 Labelled Liposomes.....	26
3.2.3 Gold Nanospheres.....	26
3.2.4 Gold Nanorods .....	26
3.2.5 PBAE Nanoparticles.....	27
3.2.6 Labelled pBAE Nanoparticles .....	28
3.2.7 Lipid-coated Gold Nanospheres and Nanorods.....	28
3.2.8 Lipid-coated pBAE Nanoparticles.....	29
3.2.8.1 Method 1 .....	29
3.2.8.2 Method 2 .....	30
<b>3.3 Size Characterization of Nanosystems</b> .....	<b>30</b>
3.3.1 Dynamic Light Scattering (DLS) .....	30
3.3.2 Nanoparticle Tracking Analysis (NTA).....	31
3.3.3 Transmission Electron Microscopy (TEM) .....	31
3.3.4 Cryo-Transmission Electron Microscopy (CryoTEM) .....	31
<b>3.4 Other Characterization Techniques</b> .....	<b>32</b>
3.4.1 Preliminary Study of Stability.....	32
3.4.2 Confocal Microscopy.....	32
<b>3.5 In vitro Cell Transfection Studies</b> .....	<b>33</b>
<b>Chapter IV: Results and discussion</b> .....	<b>34</b>
<b>4.1 Liposomes</b> .....	<b>34</b>

<b>4.2</b>	<b>Gold Nanosystems</b> .....	<b>36</b>
4.2.1	Gold Nanospheres.....	36
4.2.2	Gold Nanorods .....	37
<b>4.3</b>	<b>PBAE Nanoparticles</b> .....	<b>39</b>
4.3.1	Previous Studies.....	39
4.3.2	Physiochemical Characterization of NPs.....	40
4.3.3	Preliminary Studies of Stability .....	42
<b>4.4</b>	<b>Lipid-Coated Nanosystems</b> .....	<b>45</b>
4.4.1	Lipid-Coated Gold Nanospheres .....	46
4.4.2	Lipid-Coated Gold Nanorods.....	48
4.4.3	Lipid-Coated pBAE Nanoparticles .....	50
<b>4.5</b>	<b>Fluorescence Colocalization Experiments</b> .....	<b>53</b>
<b>4.6</b>	<b><i>In vitro</i> Cell Transfection</b> .....	<b>54</b>
<b>Chapter V: Conclusions</b> .....		<b>56</b>
<b>Chapter VI: Bibliography</b> .....		<b>59</b>

## **CHAPTER I. MOTIVATION AND AIMS**

## Chapter I. Motivations and Aims

### 1.1 Motivations

The World Health Organization defines cancer as a large group of diseases that can start in almost any organ or tissue of the body due to the uncontrolled growth of abnormal cells that go beyond their usual boundaries to invade parts of the body and/or spread to other organs, forming malignant masses and metastasis. Cancer is one of the major diseases that caused millions of deaths in the 20th century, and still remains a difficult disease to treat with more than ten million new cases every year [1]. The most common treatments for this disease are surgery, radiotherapy, chemotherapy and, lately, immunotherapy is gaining attraction.

**Surgery** is the most effective treatment for local and solid cancers but is inefficient when the cancer has spread throughout the body due to the metastasis and it is also difficult to remove all the cancerous mass and remaining tumor cells can develop a tumor easily. For this reason, surgery is often used in combination with chemotherapy and/or radiotherapy. In addition, it cannot be used in late stages of the disease, the most common diagnosed ones, when cancer is more spread. Therefore, its clinical use is limited [2].

Regarding **radiotherapy**, it consists in using ionizing radiations to radiate the tumor, leading to damages in DNA and high oxidative stress. The efficacy of radiotherapy, on the other hand is limited by the radio resistance of the tumor cells and the challenges of developing a highly precise treatment plans to deliver high radiation doses to a defined treatment volume without damaging the surrounding normal tissues [3]. In addition, as surgery, it is limited to local effects, therefore being not useful for advanced tumors.

**Chemotherapy** is, by far, the most common treatment of choice for most solid and blood tumors. In chemotherapy, the systemic administration of one or more cancer drugs is the current choice for the treatment of advanced stage or metastatic cancers, since they are able to reach every organ in the body via the bloodstream, but these drugs are based on toxic compounds that inhibit the fast proliferation of the cancer cells but also healthy cells such as hair follicles, bone marrow and gastrointestinal tract cells which leads to the undesirable side effects [4]. Even being its use so spread, the look for novel treatment approaches that focus on the reduction of side effects is an urgent need.

Among all treatments, **immunotherapy** is the one on which research has been focusing mostly on recent years as it has proven to significantly increase the long-term survival of many patients. From the patient's point of view, this is associated with a lower incidence

of side effects compared to traditional treatments. It consists in stimulating the natural defences of the body to fight against the tumor, stopping or slowing down its growth and diffusion to other tissues and enhancing the immune system to destroy it.

Several types of immunotherapy are already used in clinics to treat some cancer types, these include:

- **Monoclonal antibody therapy**, which involves the use of highly specific monoclonal antibodies (mAb), also called therapeutic antibodies, that are immune system proteins experimentally produced in the laboratory from identical immune cells and engineered to work as substitute antibodies that target only a single site (epitope) on a single antigen [5]. Some monoclonal antibodies are immunotherapeutic because they help turn the immune system against cancer. An example is *blinatumomab*, which binds to both CD19, a protein found on the surface of leukaemia cells, and CD3, a protein on the surface of T cells. This process helps the T cells get close enough to the leukaemia cells to respond to and kill them [6]. Manifold monoclonal antibodies have been approved by the FDA to fight different types of cancer, including breast, head and neck, lung, liver, bladder, and melanoma skin cancers, as well as Hodgkin lymphoma [7].
- **Anti-immune checkpoint inhibitors**, which are a type of mAb that inhibit the normal functioning of immune checkpoints. The latter are natural regulators of the immune systems found on the surface of healthy and cancerous cells and when they bind with partner proteins on T-cells they send a signal to the immune system to avoid that cells are destroyed. For example, the binding of checkpoint proteins such as PD-L1 on tumor cells and PD-1 on T cells represents an adaptive immune resistance mechanism that is exerted by tumor cells. Blocking the binding of PD-L1 to PD-1 with an anti-immune checkpoint inhibitor (anti-PD-L1 or anti-PD-1) allows the T cells to kill tumor cells with a consequent boost of the immune response [8]. The first anti-cancer drug targeting an immune checkpoint is *Ipilimumab*, approved in 2011 by the Food and Drug Administration (FDA) for treatment of melanoma [9]. Clinical trials have also shown some benefits on lung cancer or pancreatic cancer, specifically in combination with other drugs [10] [11].
- **T-cell therapy**, that uses specific immune cells, T-lymphocytes, which are extracted from a patient's blood sample, genetically modified and grown in the laboratory to then be re-infused into the patient through the veins to activate and re-educate the immune system's response. There are two main types of T-cell therapy: tumor-infiltrating lymphocytes (or TIL) therapy and CAR T-cell therapy. The first uses T lymphocytes called TIL that are in or near the tumor and are tested in the laboratory to find out which ones best recognize cancer cells to then be grown and infused in

the patient. In CAR T cell therapy, T cells are modified in the laboratory to produce a type of receptor known as CAR to allow T cells to bind specific proteins on the surface of cancer cells, improving their ability to attack cells cancer. Four CAR T-cell therapies have been approved by FDA, both for blood cancers, while treatments for cervical squamous cell carcinoma and cholangiocarcinoma are still experimental [12].

- **Cancer vaccines:** or better, cancer therapeutic vaccines, unlike prevention vaccines, can help the immune system to “learn”, recognize and react to tumor-associated antigens (TAAs) and destroy cancer cells that contain them. Vaccines for cancer can be produced in three main ways: they can be tailored to cause an immune response against specific and unique characteristics of a patient's tumor, or they can be made from TAAs found on the cancer cells of many people with a specific type of cancer, but this type of vaccine is still experimental. Finally, they can be made from dendritic cells (DC) extracted directly from the patient. A DC vaccine for advanced prostate cancer has been approved and other types of cancer vaccines have been approved to treat some melanoma that returns after surgery [13] [14].

Among all immunotherapies, we focus on the latter, more specifically on **cancer treatment vaccines** selectively targeting **dendritic cells** (DC). DCs are specific immune system antigen-presenting cells (APC) that, when they are activated, present the antigen to be destroyed on their surface stimulating an antigen-specific T-lymphocyte mediated immune response. In the last decades, several mechanisms have been proposed to load the antigen into DCs, among these the transfection of them with DNA or RNA through vectors as a **gene therapy** [15]. With this technique, nucleic acids or fragments of them, such as plasmid DNA (pDNA) and messenger RNA (mRNA), are inserted into specific cells to modulate gene expression with the aim of treating the disease [16]. Therefore, the main challenge of gene therapy is the transfection of nucleic acids within the patient's target cells, and to do this, over the years, many viral and non-viral carriers have been produced and tested [17].

For these objectives, **Nanomedicine**, as well as **Bionanotechnology**, comes into play, which in recent years has made its way between new strategies for treatment, diagnosis or both. The application of nanotechnologies for cancer treatment includes anticancer drug delivery, tumor imaging, early detection, molecular diagnosis, targeted therapy and cancer bioinformatics, but among all, their use for gene therapy purposes have been in the forefront of research laboratories [1] [18]. The nanoscopic size of nanomaterials allows the interaction with tissues at the same scale of many biological processes, enhancing the intracellular uptake, important aspect for gene delivery.

In recent decades multiple colloidal nano-scale systems containing anticancer agents

have been designed, such as small molecular weight drugs or macromolecules as genes, that fully respect the important features of biocompatibility and non-toxicity required in the interactions with biological materials [4]. Moreover, carriers should maintain their structure stable through the systemic circulation and the extracellular environment, and they should be very specific for target specific cell lineages.

Although **viral vectors** remain by far the most popular approach in gene therapy trials due to their high transfection efficiency and cell specificity [19], problems concerning safety issues and limited encapsulating capacity lead to the increasingly advanced study of synthetic **non-viral vectors**, such as lipid vesicles, polymeric and inorganic nanocarriers [18].

The advantages related to the use of **liposomes** for this therapy are manifold, above all the amphiphilic nature of their membrane whose structure, composition and proportion is analogue to the cell membrane, and gives them the abilities to envelope and protect many types of therapeutic biomolecules, both hydrophilic and hydrophobic molecules. This membrane is the result of a self-assembly of dissolved lipid molecules, each of which contains a hydrophilic head group and hydrophobic tails. For gene therapy, cationic (or neutral) lipid molecules are preferred since the positive charges favour the spontaneous electrostatic interaction with the DNA, which has negatively charged phosphate groups, for example DOTAP that is positive and DOPC neutral.

Additional advantageous properties are their low cost, biocompatibility and almost biologically inert profiles, not causing antigenic or toxic reactions in a high percentage of cases. Thanks to these dynamic properties and their relative ease of handling, liposomes have been widely used for the delivery of drugs and genes [20]. However, they have some limitations that still need to be investigated, such as problems with stability, industrial reproducibility and the limited control of the gene release [4].

In contrast, **polymeric nanoparticles** are promising carriers in cancer therapy because they have enabled the efficient delivery of therapeutic agents allowing a longer blood-stream half-life, showing reduced toxicity and improving pharmacokinetics [4].

Moreover, they represent a promising choice for gene delivery for many reasons, such as the protection and controlled release of gene materials and the ease, versatile and tailored production [18].

Among them, polyplexes have been widely studied. They are nano-sized complexes formed through the electrostatic interaction of cationic polymers and nucleic acids. Despite their significant advantages, such as low toxicity profile and promising transfection efficiency, it is important to underline that the design of highly efficient polyplexes that successfully overcome all biological barriers is still one of the main challenges in gene delivery [21]. Furthermore, one of the main problems related to

polyplexes is its limited stability, which can be strongly compromised in the presence of ions [22].

All these nanocarriers can also be designed for "**theranostic**" applications, that is, for simultaneous diagnostic and therapeutic purposes by the incorporation of **magnetic particles**, together with **therapeutic agents**, as contrast agents for imaging techniques, such as gold, silver, gadolinium and other nanoparticles, which have a low level of toxicity in physiological environments [1].

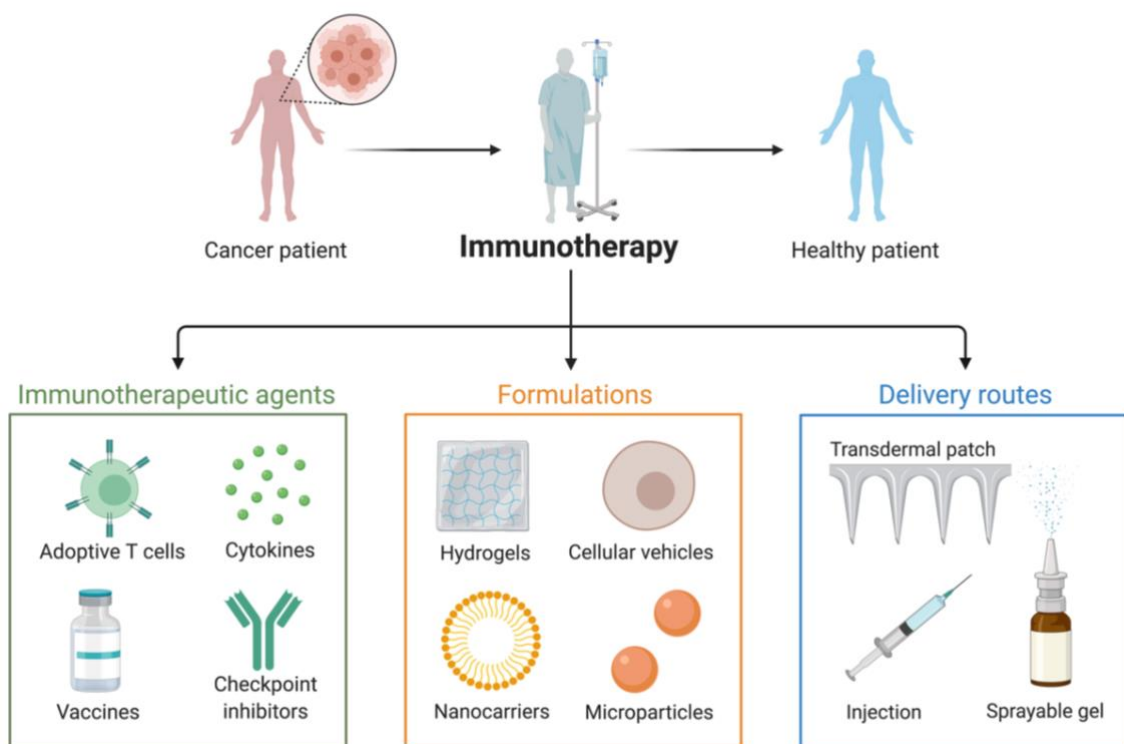


Figure 1. An overview of cancer immunotherapy approaches.

## 1.2 Aims

This thesis arises from a collaboration between Institut Químic de Sarrià (IQS) in Barcelona and Politecnico of Turin. Previously, at IQS, polymeric nanoparticles, composed of **oligopeptide end-modified poly ( $\beta$ -aminoester) (OM-pBAE)**, a class of polymers composed of ester bonds, have been developed as gene delivery systems showing high biocompatibility, biodegradability in physiological conditions and a reduced toxicity. Furthermore, they can be designed to increase their buffering capacity, and their ability to compact nucleic acids improving their capacity to promote cellular internalization. Once inside the endosomes, thanks to the proton sponge effect, endosomal escape, required for the expression of the encoded gene, is also enhanced [18]. At PoliTo, lipid nanosystems, both liposomes and natural extracellular vesicles, have been designed and re-engineered to encapsulate and/or coat **inorganic metal oxide nanoparticles**, with the aim to increase the cell penetration efficiency, biomimicry, non-immunogenicity and bio-stability of inorganic nanoparticles, such as zinc oxide (ZnO) and mesoporous silica (MSNs) nanoparticles.

Combining both expertise, the aim of this Master thesis is to lay the groundwork for the design of a mRNA cancer vaccine based on lipid nanocarriers and pBAE nanoparticles, with the purpose of making an efficient and theranostic nanosystem.

The main objective of the thesis concerns the synthesis and characterization of liposomes that encapsulate within them or interact with metallic and/or polymeric particles, in order to combine the advantages associated with pBAE polyplexes and improve their stability in the biological environment and the interaction with cells.

The main objective can be divided in the following secondary objectives:

1. Synthesis of well-characterized neutral liposomes, using the solvent exchange methods.
2. Synthesis and characterization of pBAE polyplexes, already widely studied by the GEMAT group of IQS.
3. Synthesis and characterization of gold nanosystem, investigated both for theranostic purposes but also for their stability and inertia unlike the pBAE during encapsulation.
4. Test the encapsulation of various metallic and polymeric nanoparticles inside liposomes. Lipid nanosystems produced were investigated and characterized.
5. Preliminary studies of cell culture transfection were carried out.

## **CHAPTER II. BACKGROUND**

## Chapter II. Background

As it has been stated so far, **cancer disease** continues to be a major health concern worldwide being the second leading cause of death in the world. It still remains a chronic disease to treat and also a significant cause of morbidity, due to problems caused by treatments [1]. The common treatments for cancer are surgery, radiotherapy, chemotherapy or a combination of these methods.

The most widely used is certainly **chemotherapy**, which is the administration to the patient of one or more anticancer drugs that kill dividing cancer cells and prevent them from growing by inhibiting mitosis. Unfortunately, these drugs are cytotoxic not only for cancerous cells, but they can damage also healthy tissues, especially cells of the gastrointestinal tract, bone marrow and hair follicles cells causing severe and undesirable side effects like gastrointestinal problems, among them nausea, decrease of white blood cells which causes a weakened immune system and loss of hair [4].

Moreover, the **multidrug resistance** of cancer cells is another important reason for the low efficacy of chemotherapy, therefore, in recent years, research is heavily focused on finding new effective therapies and mostly with lower incidence of side effects, among the latter **Cancer Immunotherapy** is a growing field dedicated to the development of novel cancer therapies by understanding and making use of immune pathways. The immune system keeps track of all of the macromolecules normally found in the body. Any new molecules that the immune system doesn't recognize triggers an alarm, causing the immune system to attack it.

The idea of exploiting the patient's immune system to treat cancer is based on the insight that the immune system can suppress the development or progression of spontaneous malignancies in a process called "immune surveillance" [23]. Human tumors arise from a combination of genetic changes that facilitate immortality, but at the same time create neo-antigens that are supposed to make cancer cells detectable by the immune system and target them for destruction. Unfortunately, cancer cells often manage to escape immune recognition and subsequent destruction through multiple resistance mechanisms, thus making them less immunogenic and more resistant to apoptosis [24].

Immunotherapies against existing cancers include various approaches among which vaccination with tumor antigens and the consequent augmentation of antigen

presentations to increase the ability of the patients own immune system to mount an immune response against neoplastic cells, have recently made their way among the new strategies in development [25].

## 2.1 Cancer Therapeutic Vaccines

The primary approach to specifically activate cells of the immune system against tumor antigens is **therapeutic cancer vaccination**, in addition to the **prophylactic (or preventative) vaccines** which are used with considerable success for the prevention of cancers of viral origin, such as hepatitis B virus and human papillomavirus (HPV) [26].

In contrast to prophylactic vaccines, therapeutic vaccines are designed to boost the immune system to attack a disease that already exists, especially in those cases where the tumor may relapse when a certain number of cancerous cells escape after traditional treatment and remain in the body. These cells are able to reproduce the tumor and consequently the disease becomes more difficult to eradicate.

The main goal of treatment vaccines is to stimulate antigen-specific T cell responses, particularly CD8+ cytotoxic T lymphocytes (CTLs) or T cells mediated responses, a type of white blood cell that express T-cell receptors (TCRs) which can recognize a specific antigen expressed by many different patients' tumors (tumor associated antigen, TAA). Tumor cells change the MHC-I presentation (a type of surface molecule that display peptide fragments of proteins to cytotoxic T cells) to indicate that it must be annihilated by the T-cells. If the TCR is specific for that antigen, it binds to the complex of the class I MHC molecule and the antigen, and the T cell destroys the cell [27] [28].

In the last few years, different types of cancer vaccines have been developed, these include **cell-based vaccines**, such as dendritic cell (DC) vaccines, **protein/peptide vaccines**, **viral/bacterial-based vaccines** and **oligonucleotide-based vaccines** [29]. A common feature and a critical step among these types of vaccines is the efficient presentation of cancer antigens to T cells.

In this context, cell-based vaccination represents a promising strategy for harnessing the immune system since DCs are the most efficient antigen presenting cells (APCs) and play a central role in coordinating innate and adaptive immune responses [30].

**Dendritic cells** are antigen presenting cells (also known as accessory cells) of the immune system that displays antigen complexed with major histocompatibility complexes (MHCs) on their surfaces to activates T lymphocytes (**Figure 2**).

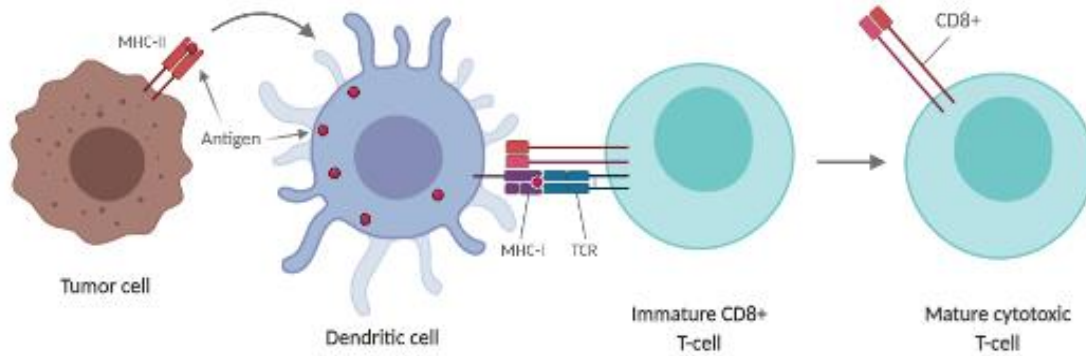


**Figure 2. Initiation of the adaptive immune response to cancer by dendritic cells.** The dendritic cells capture and process antigen material and then present it on the cell surface to activate naive T-cells. Once activated, T-cells begin proliferating and can attack cancer cells.

DC vaccines can be prepared *ex vivo* as a personalized therapy to avoid rejection of infused cells, using thus cells directly extracted from the patient, loaded with antigens and then reinfused in the patient, or *in vivo*, using efficient transfection systems that actively target DC cells directly in the patient. The latter allows for vaccines to be produced on a larger scale and for direct stimulation and activation of natural DC at multiple sites.

The main and critical issue regarding *ex vivo* DC vaccines include:

1. Selection of proper tumor antigens.
2. Choice of the appropriate strategy for loading tumor antigens onto the DCs.

Ideally, the antigen should be expressed specifically by cancer cells and not in healthy tissues, it should be present on all cancer cells such that the cancer cannot escape immune attack and finally it should be highly immunogenic [31]. As it is shown in **Figure 3**, the loading of TAAs can be made through different methods:

1. Transfection with plasmid DNA or mRNA that encodes the gene for the antigen of the protein of interest as a gene therapy, in the case of known antigens [15].
2. Pulsing DCs with known antigen proteins or peptides that form an antigen peptide/MHC complex on the cell surface with electroporation and/or sonoporation processes [32].
3. Incubation and multiple freeze-thaw cycles with lysates of autologous or allogeneic whole tumors or tumor cell lines in which unspecific antigens are present as well as known ones [33].
4. The use of hybrid cells generated by fusion of DCs and tumor cells (DC-TC) [34].

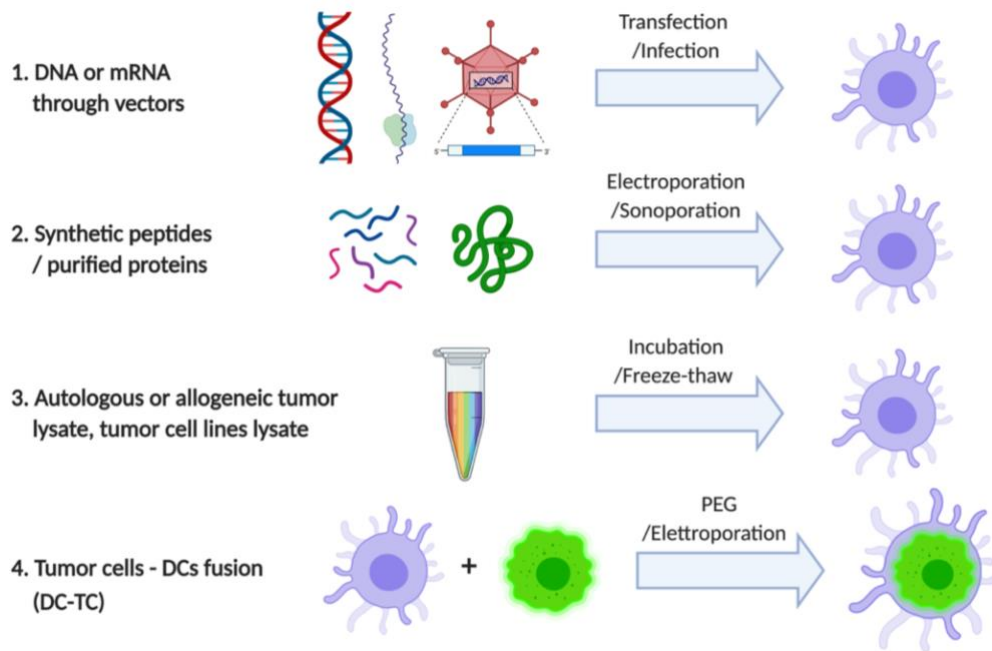


**Figure 3. Several strategies have been used to load DC with tumor antigen for antitumor immunity.** 1) DCs can be engineered with plasmid DNA or mRNA through viral or non-viral vectors to express specific gene products. 2) Synthetic peptide or purified proteins can be pulsed into DCs to form an antigen peptide/MHC complex on the cell surface. 3) Autologous or allogeneic tumor lysate and tumor cell lysates can be mixed with immature DC so that the DC will process and present multiple peptides. 4) DCs can be fused with entire tumor cells via PEG or electroporation.

In this thesis we mainly focused on the method based on the *in vivo* targeting of dendritic cells as gene therapy. After transfection with antigens, DCs express the encoded protein, which can trigger specific activation of the immune system, along with the enhancement of inflammation caused by the detection of tumor antigen as a foreign element. One of the biggest challenges concerns the transfection of nucleic acids within the patient's target cells, since nucleic acids are not capable of crossing the cell membrane due to their high negative charge and high molecular weight. They are also highly susceptible to degradation in an extracellular environment. Therefore, the protection of nucleic acids with appropriate vehicles are required for successful gene therapy [18] [35].

Regarding nucleic acids, there are different materials that can be used in gene therapy as therapeutic agents: such as **plasmid DNA (pDNA)** that requires cellular and nucleus internalization to synthesize encoded proteins as tumor antigens, and **messenger RNA (mRNA)** that instead only needs to pass the plasma membrane in order to induce protein synthesis to control gene expression. In addition, mRNA can be easily produced (**Table 1**).

**Table 1. Advantages of RNA over DNA vaccines [36].**

	DNA	RNA
Delivery	DNA needs to cross both cell and nuclear membranes and be first transcribed in the nucleus before protein expression occurs	RNA only needs to gain entry into the cytoplasm, where translation and thus protein expression directly occur
Integration	DNA vaccines are able to integrate into the host genome, which might result in insertional mutagenesis and chromosomal instability	RNA cannot integrate into the genome and therefore has no oncogenic potential
Expression	Long-term expression possible (months to years), depending on vector	Transient expression

Among DCs-based cancer vaccines, *Sipuleucel-T* has been approved by The US Food and Drug Administration (FDA) in 2010. It is composed of autologous antigen-presenting white blood cells that have been incubated with a recombinant protein consisting of granulocyte-macrophage colony-stimulating factor (GM-CSF), that helps the APCs to mature, fused to prostatic-acid phosphatase (PAP), a protein expressed by prostate cancer cells. Upon administration, the vaccine may stimulate an antitumor T-cell response against tumor cells expressing PAP. *Sipuleucel-T* has showed a survival benefit in Phase III clinical trial for patients with metastatic prostate cancer [23] [37].

Regarding cancer vaccines based on mRNA, recently CureVac, company leader in mRNA-based drug development, has developed a novel investigational therapeutic mRNA vaccine in early clinical development for the treatment of lung cancer. The CV9202 vaccine consists of six mRNAs that code for six different tumor-associated antigens designed to induce an immune response against the tumor. CV9202 and the preceding cancer vaccine CV9201, which have been investigated in two phase I/IIA trials in patients with advanced prostate cancer and non-small cell lung cancer (NSCLC), have demonstrated activity in generating cellular and humoral immune responses against the encoded antigens [38].

## 2.2 Gene Transfer Methods

As mentioned above, the major challenges in gene therapy are the delivery of the therapeutic nucleic acid into the patient's target cells. Therefore, the design of specific vectors that are able to store and preserve the gene material inside them and that are able to selectively *in vivo*-target the cells of interest, are required.

Currently, gene transfection methods can be divided in three groups: viral vectors, non-viral vectors and physical methods, including electroporation, sonoporation and microinjection. Anyway, the latter method has significant disadvantages compared to the first two which, on the other hand, have been widely studied and used for years for gene therapy [39].

**Viral Vectors** are the most common methods for gene transfer due to their high transfection efficiency and cell specificity. They are natural pathogens that have evolved over the years to protect and deliver the viral genome into cells through infection, an important property that has led to the engineering of viruses as gene delivery. Adeno-associated virus (AAV) was the first FDA-approved virus-based gene delivery vector for the treatment of a rare retinal disease. However, the potential risks of viruses, including high immunogenicity and limited gene capacity, drive the development of safe gene delivery vectors [35].

**Non-viral Vectors** are a potential alternative to viral vectors to overcome their limits thanks also to the development of new biocompatible materials. Typically, non-viral vectors can be classified in three major groups: **polymeric nanosystems** (polyplexes), **lipid nanosystems** (liposomes) and **inorganic nanoparticles**. Nucleic acids, thanks to the presence of phosphate groups, have a hydrophilic nature and a negative charge. Therefore, the formation of complexes between nucleic acids and cationic materials occurs due to an electrostatic interaction with the aim of condensing macromolecular nucleic acids into nano-sized particles, protecting nucleic acids from degradation and allowing passage through the cell membrane [35] [40].

### 2.2.1 Lipid Nanosystems

Lipid-based vectors are among the first successful systems used both for gene transfection but also for delivery of anticancer drugs. The advantages of these carriers are their ease synthesis, biocompatibility, biodegradability, safety and good reproducibility but overall, the composition of their membrane that is similar to the cell membrane and gives them the abilities to envelope and protect biomolecules, and furthermore it favours the endosomal escape that occurs through the membrane's fusion mechanism. These vectors are amphiphilic molecules composed of a non-toxic phospholipid's bilayer that form vesicles, called Liposomes (LPs), in aqueous environment. This unique structure of liposomes aids in encapsulating hydrophobic components within their lipidic bilayer, while hydrophilic components can be

encapsulated in the inner aqueous compartment [41].

They present two main domains which give them specific charge features:

1. A **hydrophilic head-group** which is responsible for condensing the negative charges of the oligonucleotide and it also provides the transfection properties.
2. A **hydrophobic tail** that influences liposomes' stability, protection of genes from degradation, endosomal escape, release from the oligonucleotide, nuclear penetration and vector toxicity [42].

The vesicles size is an important parameter in determining the circulation half-life of liposomes, and both size and number of bilayers affect the amount of molecules encapsulation in the liposomes. Therefore, LPs can be classified according to size, ranging from 20 nm up to a few  $\mu\text{m}$  in diameter, and the number of bilayers in: **Multilamellar Vesicles (MLV)**, **small or large Unilamellar Vesicles (ULV)** and **Multivesicular Vesicles (MVV)** composed of several vesicles surrounded by a single lipid layer, usually considered as MLV [43] [44] (**figure 4**).

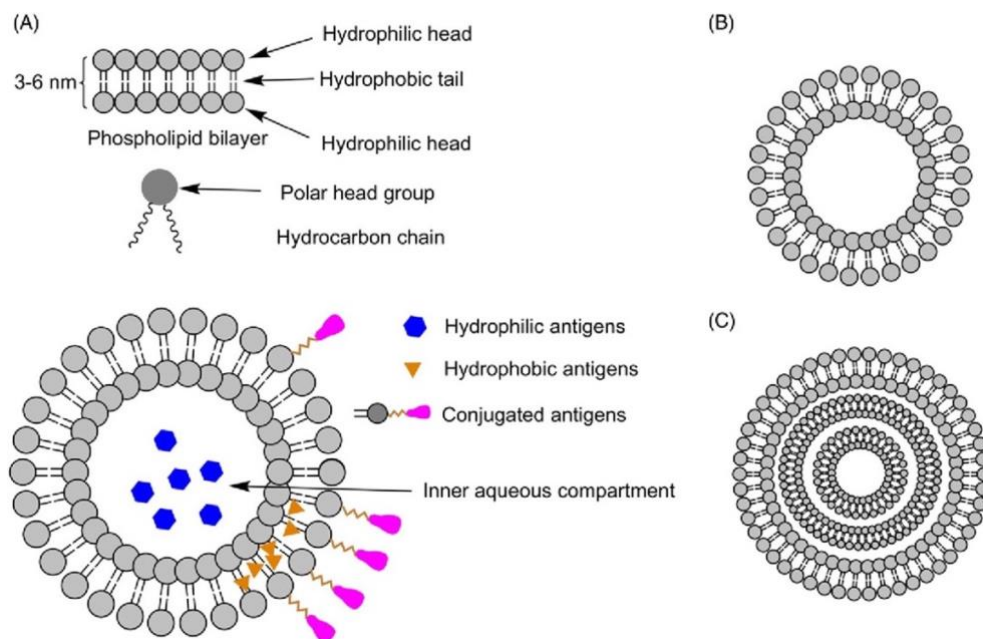


**Figure 4.** (A) Schematic representation of liposomes as an antigen delivery system. (B) Unilamellar liposomes. (C) Multilamellar liposomes [41].

For gene therapy, cationic or neutral lipid molecules are preferred since the positive charges favour the spontaneous electrostatic interaction for example DOTAP (1,2-dioleoyl-3-trimethylammonium-propane) that is positive charged and DOPC (1,2-dioleoyl-sn-glycero-3-phosphocholine) that is neutral.

**Synthesis of liposomes** can be made in two ways. The first by hydration of a thin film, in which multilamellar vesicles are prepared by hydration with aqueous buffer of a thin film obtained by evaporation under reduced pressure of a lipid solution dissolved in an organic solvent, such as chloroform. The second method involves hydration in the presence of the solvent. This method consists in the formation of an oil-in-water emulsion in which the oily phase consists of a solution of the lipid in a volatile organic solvent. Liposomes are formed following the evaporation of the organic solvent.

The first FDA approved lipid nanosystem was *Doxil*, a PEGylated liposome loaded with an anticancer drug, doxorubicin (DOX), for the treatment of AIDS-related Kaposi's sarcoma, breast cancer, ovarian cancer, and other solid tumors, and it also was the first approval for nanomedicine [45] (**Figure 5**).

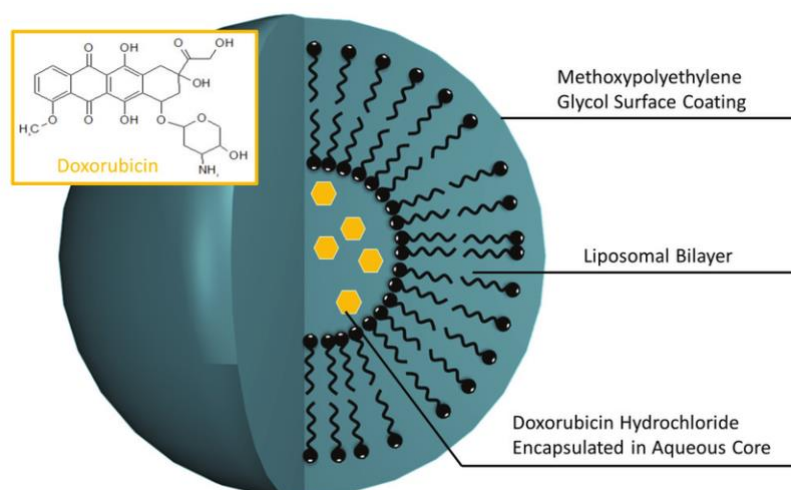


**Figure 5. Schematic of PEGylated liposomal doxorubicin (Doxil) structure.** In 1995, it was the first liposome reached commercialization with the FDA approval [46].

Despite the many advantages of liposomes listed earlier, one of the major limitations is the low stability because of the rapid clearance by the mononuclear phagocyte system (MPS), this problem can be relatively solved with the introduction of a surface modification with PEG which improves circulation time and targeting efficiency [45].

Others important disadvantages regard the limited control of the gene release because of the interactions with lipoproteins in the blood, which may cause the liposomes to leak, leading to premature antigen release and problems regarding industrial reproducibility [41].

## 2.2.2 Polymeric Nanosystems

Polymeric vectors can be **natural**, such as chitosan, or **synthetic polymers** that are the most common ones, able to condense both DNA and RNA into nanoparticles or polyplexes for gene therapy. Several polymeric nanoparticles have been approved as a drug or gene carriers. In general, cationic polymers are the most common, due to their many positive charges providing strong interactions with the oligonucleotide thus increasing its plasma viability and cellular uptake. Among these the most used are polyethyleneimine (PEI), poly(lysine) (PLL) and poly(amidoamine) dendrimer (PAMAM) [42] [35].

Although the first **polymeric transfection vector** was PLL [47], PEI is the most common polycation that has been widely used and investigated as non-viral vector and it is also considered a “gold standard” in gene transfections because it presents superior efficacy compared to other polymers [35]. However, the excessive positive charge on the polyplex surface, in both PEI and PLL, increase the toxicity, decrease the stability and consequently the cellular uptake and the endosomal escape, limiting their use in clinical applications [48]. They also present low transfection efficacy as they suffer from a poor “proton sponge effect” [42].

Usually, polymeric nanoparticles or polyplexes are internalized into cells through endocytosis and subsequently they must escape from the endosome into the cytosol to avoid degradation. To do this, they are considered to use the proton sponge effect, an osmotically induced swelling of the endosome, triggered by the proton buffering capacity of the polyplexes, which results in rupturing of the endosomal membrane [49].

In general, all the different polycations have shown a high cytotoxicity and low transfection efficacies. This leads to the emerge of a new polymeric delivery system based on a new family of biodegradable polymers that overcome all these limits, called **Poly ( $\beta$ -aminoester)s (pBAE)**.

### 2.2.2.1 Poly ( $\beta$ -amino ester)s (pBAE)

PBAEs were discovered in the 1970s, but only in 2000 David M. Lynn introduced the name poly( $\beta$ -amino ester) [50]. These polymers are a promising class of non-viral polymeric gene delivery systems due to their significant advantages and their easy way to synthesize them. Among the main characteristics of these polymers we find high biocompatibility, reduced cytotoxicity and also high biodegradation via hydrolytically degradable ester groups. Moreover, the most interesting feature of

pBAE, that overcomes the limitations of previous polymers, is the high transfection efficacy and the subsequent escape from endosome through the proton sponge effect, due to their high buffering capacity. This mechanism allows the release of the polyplexes in the cytoplasm and as the pBAE is a biodegradable polymer this will be degraded by enzymes and consequently the release of the DNA/RNA happens [22] [51].

The structure of PBAE is characterized by the repetition of ester groups which are responsible for the high biodegradability whereas tertiary amines allow the improved endosomal escape. Moreover, the R' (radicals) can be modified in order to modify the characteristics of the polymer (**Figure 6**).

In this project we are going to use the C6 pBAE where the amines used as a radical are the 5-aminopentanol and hexylamine in a 50/50 ratio.

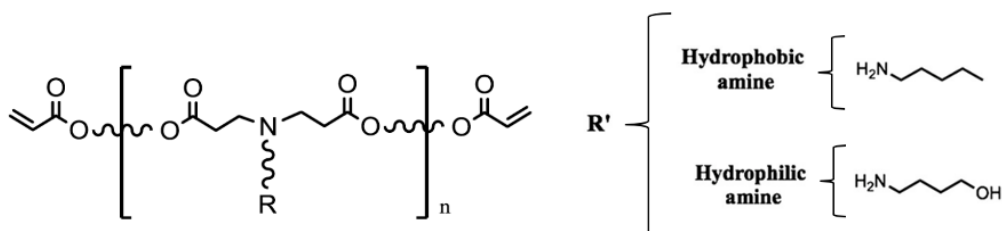


**Figure 6. Poly( $\beta$ -aminoester)s (pBAE) chemical structure.**

In addition, the GEMAT group has recently developed a family of pBAE polymers with oligopeptide-modified termini (OM-pBAEs) which are able to produce nanoparticles with an increased transfection efficiency in cell-type-specific manner and excellent biocompatibility. In particular, the modifications are based on end-capping groups modified using different **positive oligopeptides** such as Cys-Lys-Lys-Lys (C6-CK<sub>3</sub>), Cys-His-His-His (C6-CH<sub>3</sub>), Cys-Arg-Arg-Arg (C6-CR<sub>3</sub>) [52] [53].

Although this new family of pBAE polymers is promising for gene delivery due to their ability to condense nucleic acids into discrete nanoparticles, they also have limited applicability owing to rapid degradation via hydrolytic cleavage of ester bonds and thus cannot provide sustained delivery [54] and therefore, one of the main problems related to polyplexes is its limited stability, which can be strongly compromised in the presence of ions [22].

## 2.3 Inorganic Nanoparticles in Cancer Treatment

As mentioned before, among the non-viral vectors for the delivery of oligonucleotides the inorganic particles have attracted much attention due to their electronic, optical and magnetic properties not only for cancer treatment but also for diagnosis or both [55].

In the last decade, **inorganic nanoparticles (INPs)** have been extensively investigated in preclinical and clinical studies for the detection, diagnosis and treatment of many diseases due to their many advantageous characteristics. They can be used for the encapsulation and/or cargo binding, allowing NPs to recognize the tumor, permit imaging, deliver therapeutic agents and kill tumor cells [56]. In general, inorganic NPs show unique physicochemical properties; they are biocompatible, stable to storage, and often they possess optical and magnetic properties. They are inert against microbial attack and can be easily synthesized.

Despite the considerable advantages, their efficacy in gene transfection remains very low and they are often toxic, therefore surface modifications are necessary to improve their transfection characteristics, toxicity and electrostatic interactions [42].

Parameters that affect the properties are:

- a. **Size:** affects the bio-distribution and blood circulation lifetime, as well as their cellular absorption. If INPs are too big, they are captured by the liver, instead if they are too small, below 10 nm, they are eliminated by renal clearance. Small NPs have a more even distribution in tumors than large NPs, as they tend to accumulate in tumors due to the enhanced permeability and retention effect (EPR) (**Figure 7**).
- b. **Surface charge:** NPs should have a positive surface charge to be internalized and to interact with the strongly negative membrane of cancer cells. The latter tends to be further negatively charged in cancer cells due to the increased glycoprotein content.
- c. **Surface Material:** NP coatings are particularly important for active targeting; thus, NPs are functionalized with specific molecules that interact with receptors known to be selectively present in cancer cells [56].

Nowadays different types of INPs have been developed for many applications; a list of inorganic nanoparticles is shown in **Figure 8**.

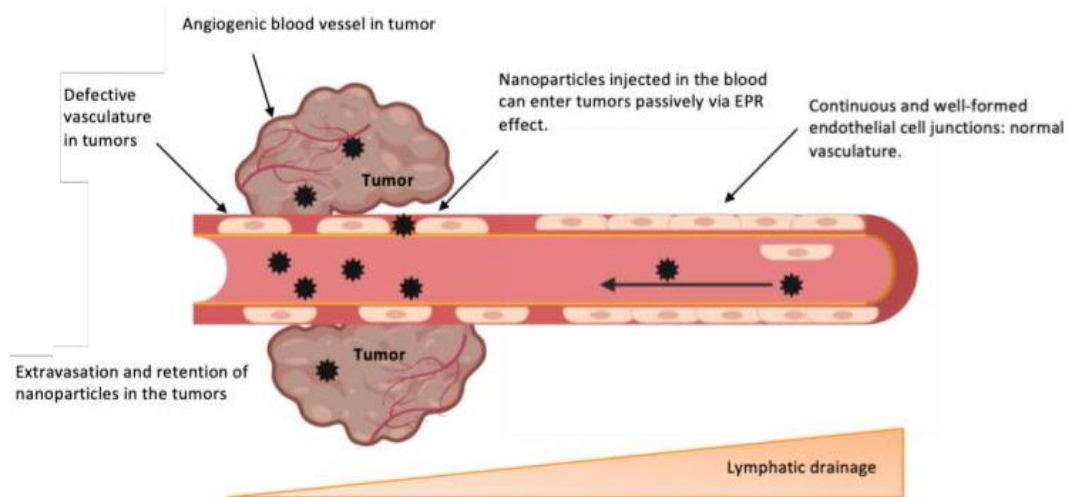


**Figure 7. Enhanced permeability and retention (EPR) effect.** Passive targeting to tumor tissue is achieved by extravasation of nanoparticles through the increased permeability of the tumor vasculature and ineffective lymphatic drainage.

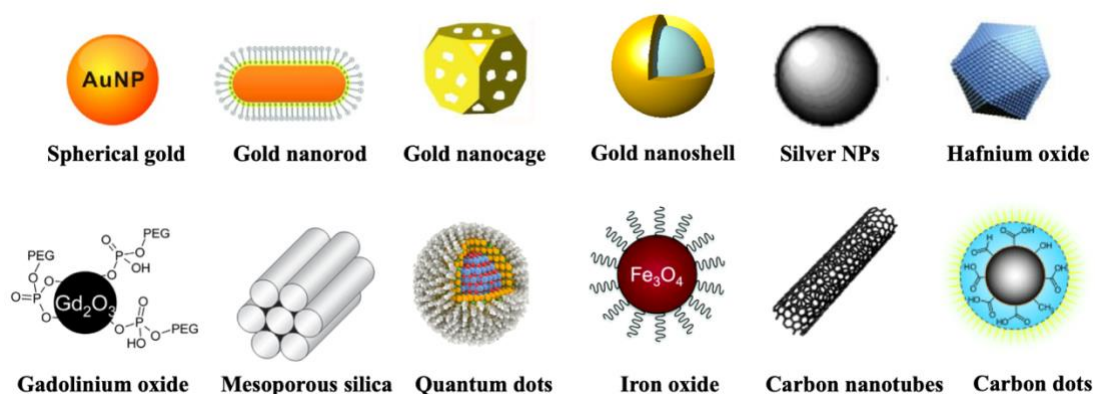


**Figure 8. Different types of inorganic nanoparticles [56].**

### 2.3.1 Gold Nanoparticles

Gold Nanoparticles, both **spherical (AuNSs)** and **rod-shaped (AuNRs)**, are among the most studied inorganic systems for applications in therapy and diagnosis because of their physio-chemical properties and its relative non-toxic nature.

Regarding optoelectronic properties, they arise from the localized surface plasmon resonance (LSPR) which is responsible for the colour of the colloidal AuNPs solution and is influenced by their size and shape. For example, gold nanospheres with a size of 10-20 nm show an absorption around 520 nm and have a red coloured solution. By changing the particle size to form nanorods, the SPR wavelength can be increased in the near infrared (NIR) region. This feature is useful for optical imaging

and photothermal therapy for cancer treatment [56]. This last application has been the focus of much research in the medical field. The Au nanorods are synthesized and superficially modified to selectively bind to the surface of malignant cancer cells, aiming to kill them through a selective localized photothermal heating.

Regarding chemical and biochemical properties, gold has been shown to have a strong affinity for thiols and amines, therefore, this allows for easy surface modifications with many different biological ligands, such as DNA, peptides, proteins, antibodies, viruses and receptors [57].

Among the simplest and most used methods for the **synthesis** of nanosphers we find the chemical reduction method and, as regards the nanorods, a seed-mediated method. The synthesis is scalable and usually provide small dispersion nanoparticles, around 10-20 nm, and are therefore easily internalized by cells [58] [59].

### 2.3.2 Zinc-oxide Nanoparticles

Zinc-oxide Nanoparticles (ZnO NPs) are believed to be nontoxic, biosafe and biocompatible INPs and furthermore, they possess potential intrinsic anticancer characteristics.

The cytotoxicity of ZnO is related either to its rapid dissolution and release of cations inside the cell and to the production of ROS (Reactive Oxygen Species) under specific conditions which can lead to cell death when it exceeds the antioxidant capacity of the cell causing oxidative stress and the subsequent damage of cells DNA. This important cytotoxic behaviour for cancer cells is caused by a high concentration of zinc and selective targeting towards cancer cells which make it an anticancer agent [60] [61].

However, in most cases, it is not clear whether ZnO dissolution occurs in the extracellular medium or after cell internalization. Therefore, V. Cauda and her group at PoliTo demonstrated that engineering the surface of ZnO NPs with a lipidic bilayer leads to an enhancement of the colloidal and chemical stability in biological media. Moreover, these properties are related to an appreciable enhancement of cellular internalization of this new hybrid nanoconstruct [62].

### 2.3.3 Mesoporous-silica Nanoparticles

Mesoporous-silica Nanoparticles (MSNs) are stable colloidal suspensions capable of

efficiently encapsulating different types of molecules within pores present on its large surface. An important challenge in current development is the design of controlled cap systems to prevent the uncontrolled and premature release of the drug from the mesopores. These pore-cap systems should also have more specific functions, such as biocompatibility and possibly containing specific ligands for cell targeting.

For this purpose, as in the case of ZnO nanoparticles, an alternative design involves the use of supported lipid bilayers (SLBs) to coat mesoporous nanoparticles. The lipid membrane can increase circulation time and accumulation in cancer cells. In addition, it improves their biocompatibility, toxicity, immunogenicity and allows cell transfection.

V. Cauda and his collaborators demonstrated the efficient preparation of SLB @ CMS, which are single colloidal mesoporous silica nanoparticles (CMS) coated with an intact supported lipid bilayer (SLB) using a solvent exchange method and neutral lipids. The principle relies on the fact that lipids dissolved in ethanolic solution prevail as monomers, while they self-assemble into solid surface-supported bilayers or liposomes as the water content of the solution is slowly increased [63].

These recent studies, conducted on both ZnO NPs and CMS, have obtained remarkable results *in vitro* and they demonstrate the potential for release of anticancer drugs or other molecules of these new nanosystems covered by a lipid bilayer or liposomes as they improve their stability in biological environment and interaction with cells.

### **2.3.4 Superparamagnetic iron-oxide Nanoparticles (SPIONs)**

SPIONs are small nontoxic superparamagnetic particles that have gained significant attention for their promising performance in diagnostics and therapy delivery [64]. Thanks to the superparamagnetic properties of the iron oxide core at nanoscale sizes, SPIONs have overcome some of the most relevant limitations in the targeted delivery of nanovehicles for biomedical applications as they can be guided and accumulated in specific tissues with the application of external magnetic fields [65]. These magnetic properties can be an important diagnostic tool as the SPIONs can be injected as contrast agents for magnetic resonance imaging (MRI) and be localized to the desired region by applying the local magnetic fields significantly increasing the resolution of existing diagnostic techniques [66]. Furthermore, localized magnetic hyperthermia can also be produced when an organ/tissue loaded with nanoparticles is exposed to electromagnetic radiation. The local heat generated

is sufficient for killing cancerous cells [67].

In general, SPIONs range in size from 1 to 100 nm and their safety profile has already been approved by the FDA and the EMA for use in humans. However, must be coated with polymers, such as polyethylene glycol (PEG), to avoid aggregation and increase colloidal stability and biocompatibility [68]. Furthermore, the use of cationic lipids or polymers for surface modification of SPIONs allows efficient binding of nucleic acids or negatively charged drugs, for a delivery system driven by an external magnetic field [69] [70]. Nevertheless, an efficient and controlled cellular internalization, as well as a stable intracellular accumulation of SPIONs, are the main challenges for these magnetic nanosystems [65].

In 2019, the group of GEMAT developed and studied polymeric nanosystems for the transport of nucleic acids and that contain in three different ways the SPIONs, since thanks to their magnetic feature, they allow cell selection. Surprisingly, these studies have shown that the presence of SPIONs on OM-pBAE/pDNA polyplexes has an enhancing effect on the transfection of both permissive and transfection reluctant cell lines, together with the allowance to perform a selective magnetic sorting of genetically modified cells (**Figure 9**) [52].

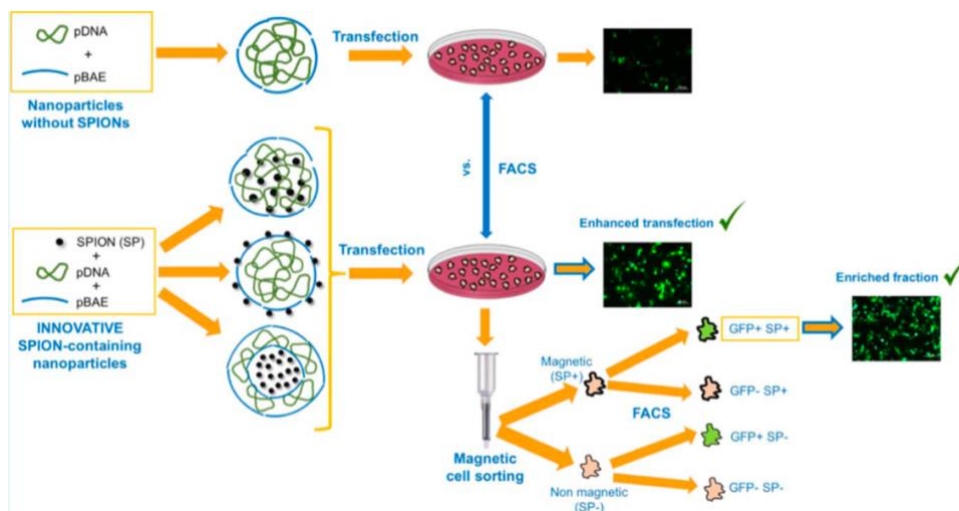


**Figure 9.** SPIONs' enhancer effect on cell transfection with OM-pBAE/pDNA polyplexes and the possibility of performing selective magnetic sorting of genetically modified cells [52].

Another example of SPIONs in cancer treatment, in 2010 there was EU-wide regulatory approval for *Nanotherm*, the magnetic therapy fluid from MagForce, consists of aminosilane-coated iron oxide nanoparticles in an aqueous dispersion designed for tumor therapy (glioblastoma) using local tissue hyperthermia [71] [72].

## 2.4 Theranostic Systems

All of these nanosystems previously listed and briefly described can be designed for “**theranostic**” applications. In 2002, “theranostic” was coined by Funkhouser and is a combination of the terms “**therapeutics**” and “**diagnostics**” [73].

Theranostic nanomedicine is emerging as a promising therapeutic model. It takes advantage of the high capacity of nanoplateforms to bring cargo and loads onto them for both imaging and therapeutic functions. The resulting nanosystems, capable of diagnosis, drug delivery, and monitoring of therapeutic response are expected to play a significant role in the dawning era of personalized medicine, and much research effort has been devoted toward that goal [74].

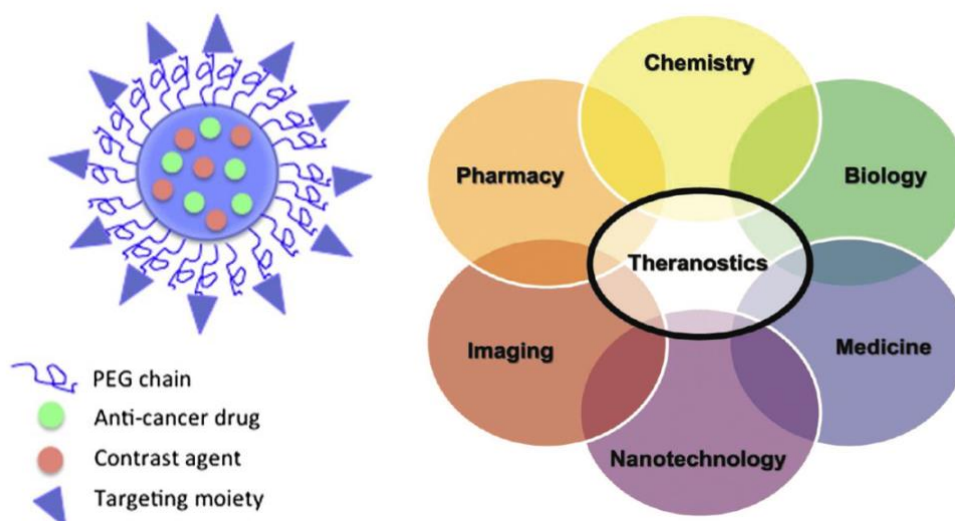


**Figure 10. Theranostics.** Schematic representation of a theranostic multifunctional nanomedicine and of the interdisciplinary field of theranostics. Theranostics are nanomedicine formulations which aim to combine disease diagnosis and therapy, and which are developed and tested by researchers working at the intersection of several different scientific fields [75] [76].

Many inorganic materials and polymer-based nanomaterials have been shown to act efficiently as an imaging agent and carrier/delivery agent. Among metallic nanoparticles we find above all SPIONs and AuNPs, that with proper surface functionalization they can also be applied in cancer theranostics.

Theranostic nanoparticles with gold can be made conjugated with other metal nanoparticles such as SPIONs, to provide multi-imaging modalities and dual therapeutic results. A recent study demonstrated remarkable results in terms of imaging, therapeutic and prognostic benefits for a novel theranostic nanosystem consisting of gold nanoparticles and SPIONs encapsulated in the hydrophobic core

of a polymer micelle. Biodegradable polymers were employed because solubility and biocompatibility were improved and also provided a site for biomolecule conjugation [77].

In conclusion, the conjugation of polymeric, metallic and lipid biomaterials bringing molecules in a single hybrid nanosystem represents an important and interesting innovation for the future of nanomedicine for the diagnosis and treatment of cancer as well as many other diseases that are difficult to treat and diagnose.

## **CHAPTER III. MATERIALS AND METHODS**

## Chapter III. Materials and Methods

### 3.1 Materials

All the reagents and solvent used for synthesis of pBAE were purchased from SigmaAldrich. CK<sub>3</sub> (NH<sub>2</sub>-Cys-Lys-Lys-Lys-COOH) and CH<sub>3</sub> (NH<sub>2</sub>-Cys-His-His-His-COOH) peptides were obtained from Ontores Biotechnologies with a purity at least 98%. Cyanine dyes used for fluorescent nanoparticles were purchased from Lumiprobe. Lipids, POPC (1-palmitoyl-2-oleoyl-glycero-3-phosphocholine) and DOPC (1,2-dioleoyl-sn-glycero-3-phosphocholine) were both from Avanti Polar Lipids and the phospholipid NBD-PE for fluorescent liposomes was purchased from ThermoFischer. Paraformaldehyde (PFA), glucose, sucrose, AcONa, Hepes, DEPC treated water, PBS were purchase from Sigma-Aldrich. Fetal bovine serum (FBS), Duplecco's Modified Eagle's Medium (DMEM), Trypsine-EDTA glutamine, penicillin and streptomycin were purchased from Gibco. Plasmid pGFP was produced and purified from *E. coli*. For the synthesis of Gold Nanospheres and Nanorods: chloroauric acid (HAuCl<sub>4</sub>) was from Supelco, trisodium citrate dihydrate (Na<sub>3</sub>C<sub>6</sub>H<sub>5</sub>O<sub>7</sub>), hexadecyltrimethylammonium bromide CTAB (CH<sub>3</sub>(CH<sub>2</sub>)<sub>15</sub>N(Br)(CH<sub>3</sub>)<sub>3</sub>), sodium borohydride (NaBH<sub>4</sub>), silver nitrate (AgNO<sub>3</sub>) and ascorbic acid (C<sub>6</sub>H<sub>8</sub>O<sub>6</sub>) was from Sigma-Aldrich.

### 3.2 Synthesis of Nanosystems

#### 3.2.1 Liposomes

In this thesis, we used a **solvent exchange method** to prepare liposomes and lipid membranes for metallic and/or polymeric nanoparticles, already tested for ZnO Nanocrystals [62] and Mesoporous Silica Nanoparticles [63]. In this process, the amount of solvent (isopropanol or ethanol for example), in which the lipids are dissolved, is continuously varied by the addition of water. The approach is inspired by the **reverse-phase evaporation method**, in which liposomes are produced through the slow removal of organic solvent from a water-solvent mixture. The principle is based on the fact that lipids dissolved in ethanol solution prevail as monomers, while they self-assemble into micelles or liposomes when the water content of the solution is increased to nearly 100%. [78].

For the synthesis of empty liposomes, the solvent exchange method was tested, and

different samples were prepared with a different amount of organic solvent. The two most commonly used neutral phospholipids were chosen for liposome formulations.

- a. 250  $\mu\text{L}$  of **POPC** in chloroform at the concentration of 10 mg/mL desiccated in the rotary evaporator and rehydrated with 1 mL of 60% v/v of milliQ water and 40% v/v EtOH forming a lipid solution. Then at 100  $\mu\text{L}$  of the lipid solution were added 700  $\mu\text{L}$  of milliQ water.
- b. 2.5 mg of **DOPC** in powder diluted with chloroform, to obtain the concentration of 10 mg/mL, desiccated and rehydrated with 1 mL of 80% v/v of milliQ water and 20% v/v EtOH. At 100  $\mu\text{L}$  of the lipid solution were added 700  $\mu\text{L}$  of milliQ water.
- c. Optional purification steps include: 30 seconds of immersion in a ultrasonication bath at 40kHz and filtration with a polyvinylidene fluoride (PVDF) syringe filter, with pore size 0.22  $\mu\text{m}$  to obtain small monodisperse liposomes (size < 220 nm) (**Figure 11**).

Once liposomes have been formed, maintaining the physical properties of the particles can be difficult since size distribution can change due to degradation of the components. Lipid suspensions should not be frozen as the freezing process could fracture or rupture the vesicles leading to a change in size distribution and loss of internal contents. Therefore, liposomes can be stored at 4-8°C for no longer than ~ 5-7 days. However, it is preferable to use fresh samples for experiments and characterizations.

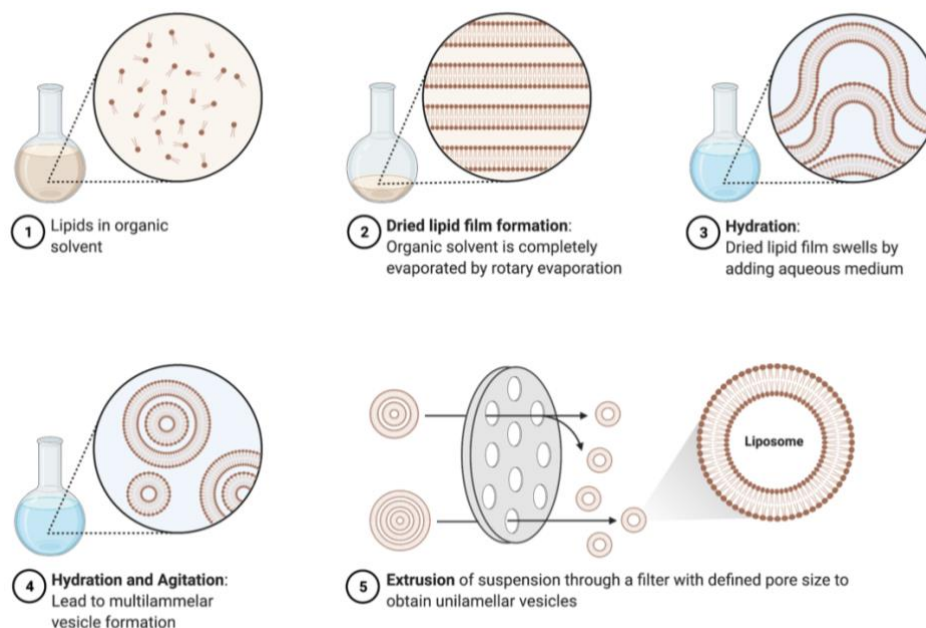


**Figure 11. Schematic representation of Liposomes preparation.**

### 3.2.2 Labelled Liposomes

For fluorescence experiments, a labelling step was added to the synthesis. Liposomes were labelled with NBD-PE (a phospholipid labelled on the head group with the environment sensitive fluorophore NBD: excitation / emission max ~463/536 nm) by adding 0,5  $\mu\text{L}$  of fluorescent dye in chloroform at 100  $\mu\text{L}$  of unlabelled DOPC before the evaporation step in the rotary evaporator.

### 3.2.3 Gold Nanospheres

Synthesis of Gold Nanospheres (AuNSs) was carried out using a **chemical reduction method** to obtain spherical particles with a size of 20 – 40 nm. This method was first proposed in 1951 by Turkevich for the preparation of monodisperse colloidal gold solutions [79]. Chemical reduction in solution is among the most widely used methods: a salt of gold is converted to metallic gold by the action of a reducing agent, a stabilizing agent that prevents the aggregation of particles, such as sodium citrate (**Figure 12**). Steps for the synthesis are: 0,5 mL of 10 mg/mL chloroauric acid ( $\text{HAuCl}_4 \cdot 3\text{H}_2\text{O}$ ) solution is heated to boiling while slowly stirring in a beaker with 49,5 mL of milliQ water. Then 1 mL of 10 mg/mL trisodium citrate dihydrate ( $\text{Na}_3\text{C}_6\text{H}_5\text{O}_7 \cdot 2\text{H}_2\text{O}$ ) is added to the auric solution. Maintain the temperature of the reaction mixture at  $100^\circ\text{C}$  until the colour changes from yellow to black and then to red or purple depending on the size of the nanoparticles. The solution prepared in this way should have a dispersion of ~20 nm and a red colour. Before the usage, 1 mL of sample is centrifuged at 13500 g for 10 minutes in a special non-stick Eppendorf to avoid the aggregation during the centrifugation.

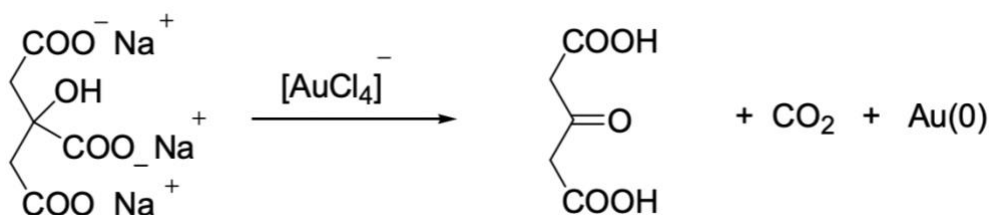


**Figure 12.** Chemical reaction of reduction of a gold salt by the action of a reducing agent such as sodium citrate.

### 3.2.4 Gold Nanorods

One of the simplest methods for production of gold nanorods (AuNRs) in solution is the **seed-mediated approach**, where nanorods are grown from small spherical gold

nanoparticles. The method consists of two stages namely seeding and growth process. Briefly, the **seed solution** was first prepared by dissolving surfactant hexadecyltrimethylammonium bromide (CTAB 136,5 mg) in milliQ water (3,75 mL) with mild stirring and slight heating until the solution was transparent. Surfactant served to direct growth of the seeds along one axis forming rods [80]. To the stirred solution, chloroauric acid ( $\text{HAuCl}_4$ , 125  $\mu\text{L}$ , 10 mM) was added, and the gold was reduced with sodium borohydride ( $\text{NaBH}_4$ , 300  $\mu\text{L}$ , 0.1 M). The seed solution was stirred for 5 minutes until the colour changed from yellow to brown and it was kept at room temperature. The **growth solution** was prepared by dissolving CTAB (7,745 g) in milliQ water (212,5 mL) with mild stirring and slight heating. Then  $\text{HAuCl}_4$  (10 mL, 10 mM) was added yielding a clear, bronze-coloured solution. Then silver nitrate ( $\text{AgNO}_3$ , 4,25 mL, 4 mM) was added, and gold was reduced with ascorbic acid (AA, 5,8 mL, 79 mM) yielding a clear, colourless solution. Finally seed solution (480  $\mu\text{L}$ ) was injected in the growth one. The mixed solution was left covered with parafilm overnight at room temperature. Samples of gold nanorods, before being used, were cleaned with two successive centrifugations at 8000 g for 8 minutes and diluted to their original volume in milliQ water (**Figure 13**).



**Figure 13.** On the left side of the picture, we find all the materials diluted to obtain the desired concentrations and the brown seed solution; on the right the AuNRs solution before and after centrifugation steps.

### 3.2.5 PBAE Nanoparticles

Polyplexes were prepared using poly ( $\beta$ -amino esters) (PBAEs) based on C6 and modified with **lysine (C6CK3)**, **histidine (C6CH3)** or **arginine (C6CR3)**, as described previously [51]. Equal volume of pBAE and DNA or RNA were mixed at

different polymer-to-DNA or polymer-to-RNA ratio (w/w) to obtain the desired polyplexes and size. Usually, the weight ratio (w/w) used in this thesis for pBAE NPs is **25:1** OM-pBAE: Nucleic acid or **50:1** to obtain smaller particles.

The nanoparticles were prepared, for example, at a ratio of 25:1 OM-pBAE: Nucleic acid, by mixing equal volumes of RNA or pGFP (green fluorescent protein-based plasmid) at the concentration of 0.5 mg/ml with the polymer (being the polymer a KH formulation, a mixture of 60% C6CK3 and 40% of C6CH3) at 12.5 mg/ml in a solution of sodium acetate (NaOAc, 12.5 mM) at a pH of 5.2. The nucleic acid was added over the polymer solution, mixed by pipetting, followed by 30 min of incubation at room temperature (v1). At this point the nucleic acid concentration and pBAE concentration is half diluted. The nucleic acid fraction was RNA or pGFP as required by the experiment. For the formation of discrete structures, the mixture (v1) after the incubation was nanoprecipitate in a same volume (v1) of RNase free water. Thereafter, the same volume (v1) of a HEPES 20 mM + 4 wt% sucrose (pH 7.4) solution was also added as cryo and lyoprotectors. At this point the sample has been diluted 3X. Then, polyplexes were lyophilized and stored at  $-20\text{ }^{\circ}\text{C}$ . On the day of use, they were redispersed in the initial preparation volume of DEPC water (v1).

### 3.2.6 Labelled pBAE Nanoparticles

For fluorescent experiments, synthesis of fluorescent pBAE NPs was carried out using labelled C6 pBAE with Cyanine5 (Cy5) and pGFP labelled with Cyanine3 (Cy3). Nanoparticles were prepared as described above, with C6 RH (60% - 40%) with 1% of Cy5 polymer (Cy5 is fluorescent in the red region: ~650 excitation, 670 nm emission) and pGFP with 1% of Cy3 (Cy3 fluoresces greenish yellow: ~550 nm excitation, ~570 nm emission).

### 3.2.7 Lipid-coated Gold Nanospheres and Nanorods

The protocol for preparing lipid-coated **metallic nanoparticles** following the solvent exchange method is:

1. 2.5 mg of **DOPC/POPC** in chloroform at the concentration 25 mg/mL in a small round flask.
2. Flask attached to a rotary vacuum evaporator that is connected to a gas pressure regulator (vacuum for chloroform at pressure 474 mbar). Level of the flask adjusted to ensure that the lipid mixture is below the water level in a preheated

37/40°C water bath and flask rotated at 120 rpm.

3. Sample dried until chloroform is totally evaporated. The lipid mixture forms a thin and uniform film on the side of the flask.
4. Rehydration of the thin film in a 1 mL mixture of **40% v/v EtOH and 60% v/v milliQ water** to form a lipid solution.
5. For **Gold Nanorods**, after the two steps of washing with milliQ water, an Eppendorf of 1 mL of sample at the concentration of  $2 \times 10^{11}$  particles/mL was centrifuged at 8000 g for 10 min and the pellet was resuspended in 100  $\mu$ L of lipid solution.
6. For 1 mL of **Gold Nanospheres** at the concentration of  $2,7 \times 10^{10}$  particles/mL, a special non-stick Eppendorf was used to avoid the aggregation during the centrifugation at 13500 g for 10 minutes and the pellet was resuspended in 100  $\mu$ L of lipid solution.
7. **Addition of water** up to 95% v/v (700 mL) results in the formation of a supported lipid bilayer on the surface of nanoparticles or liposomes.
8. From the remaining lipid solution, 100  $\mu$ L of it was diluted with milliQ water (700  $\mu$ L) to form **empty liposome** for the comparison.
9. Moreover, a **physical mixture** of metallic particles and liposomes was made to compare their interaction (as they are separated) with respect to their interaction when they are encapsulated.

### 3.2.8 Lipid-coated pBAE Nanoparticles

Two different methods of encapsulation of pBAE nanoparticles in liposomes were developed and evaluated, as a variation of the solvent exchange method (**Figure 14**). An optional purification step was added for these lipid nanosystems: 30 seconds of immersion in a ultrasonication bath at 40kHz and filtration with a polyvinylidene fluoride (PVDF) syringe filter, with pore size 0.22/0.45  $\mu$ m.

#### 3.2.8.1 Method 1

100  $\mu$ L of lipid solution (prepared with 2.5 mg of dried DOPC/POPC dispersed in 1 mL of 80% v/v of milliQ water and 20% v/v of EtOH) was used for the redispersion of a batch (50  $\mu$ L) of lyophilized pBAE NPs in which the concentration of plasmid is 0,25 mg/mL. The addition of 700 mL of water should be result in the formation of a

supported lipid bilayer on the surface of NPs or in an interaction between them and liposomes.

### 3.2.8.2 Method 2

Lyophilized pBAE nanoparticles (0,25 mg/mL of pGFP) were resuspended in a volume of 1 mL of milliQ water (or 150  $\mu$ L of fresh NPs in which the concentration of pGFP is diluted 3X, + 850  $\mu$ L of water) and this colloidal solution was used to rehydrate the lipid film in the round flask after the evaporation of the chloroform. Therefore, in this variation, ethanol is completely replaced with 100% v/v of milliQ water.

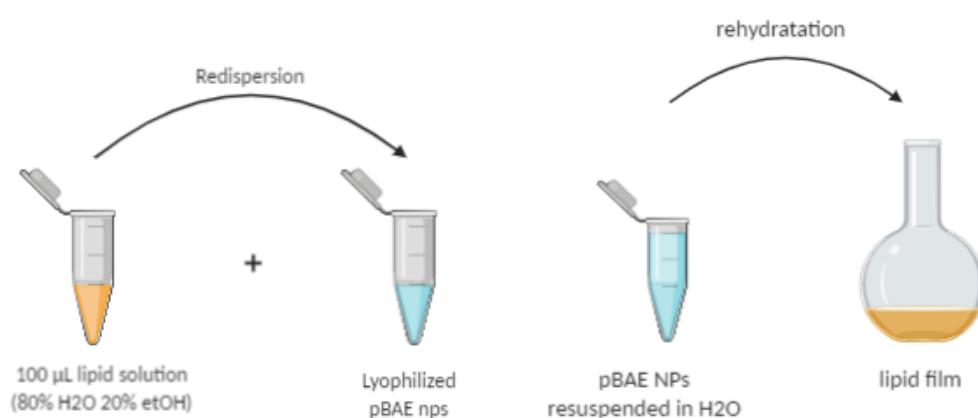


**Figure 14.** On the left, a schematic representation of the first method implemented, on the right the second one.

## 3.3 Size Characterization of Nanosystems

### 3.3.1 Dynamic Light Scattering (DLS)

PBAE Nanoparticles were characterized in terms of particles hydrodynamic size distribution, polydispersity index (PDI) and surface charge by dynamic light scattering (DLS) at room temperature with Nanosizer ZS instrument (Malvern Instruments Ltd, United Kingdom, 4mW laser). For size measurements, nanoparticles prepared at 0.25 mg/ml of RNA/pGFP were used, while for the measurement surface charge a dilution 1/10 in miliQ water (final concentration 0.025 mg/ml) was done. The value was recorded as the mean of three measurements at 173° scattering detector, and each measurement was determined from the average of 20 cycles in a disposable plastic cuvette. For lipid nanosystems and liposomes, DLS was not used as it is not suitable for highly polydisperse samples.

### 3.3.2 Nanoparticle Tracking Analysis (NTA)

Nanoparticle Tracking Analysis uses the properties of light scattering and Brownian motion to obtain the particle size distribution of samples in liquid suspension. A laser beam crosses a thin and microfluidic sample chamber and the particles suspension, and they can be visualized via long working distance, x100 magnification microscope onto which is mounted a video camera. The camera captures the Brownian motion of the nanoparticles and the software tracks many nanoparticles individually and using the Stokes-Einstein equation calculates their hydrodynamic diameters. This measurement provides the particles size and their concentration. The instrument used is NanoSight LM10 (Malvern Panalytical), based on the NTA technology and it allows rapid and accurate analysis of the size distribution and concentration of all types of nanoparticles from 10–1000 nm in diameter.

For NTA measurements of liposomes, pBAE nanoparticles, lipidic nanosystems, a dilution 1/100 in miliQ water was done for all the samples. Furthermore, measurements were also made before and after the sonication and filtration steps. For gold nanosystems, instead, samples were diluted 1/10 or 1/100.

### 3.3.3 Transmission Electron Microscopy (TEM)

Size and morphology of gold nanospheres and nanorods were measured with the transmission electron microscopy (TEM) technique. The functioning of TEM is based on an electron beam which, under vacuum, is transmitted through the sample. AuNRs samples were prepared for the TEM by centrifugation at 8000 g for 10 minutes, removal of supernatant, washing with miliQ water, and repeating. This final solution was placed on a carbon-coated copper grid and the water was allowed to evaporate. After imaging, aspect ratios were determined by measuring the length and diameter of at least 30 rods randomly selected.

### 3.3.4 Cryo-Transmission Electron Microscopy (CryoTEM)

With CryoTEM we mean transmission electron microscopy of thin vitrified aqueous films, kept at liquid nitrogen temperature [81]. It allows a virtually artifact-free depiction of very small structures in the size range from 5 nm to 200-300 nm. The aqueous samples are brought on a grid and the small liquid film is rapidly frozen to 90 K, so that ice crystals do not form, and the frozen water film remains transparent

in an amorphous state. Using Cryo-TEM we evaluate the size, size distribution, and morphology of liposomes, pBAE nanoparticles after lyophilization and lipid-coated nanosystems. Cryo-TEM is preferred for polymeric nanosystems, as well as liposomes, because some materials, particularly biomolecules, are not compatible with the high-vacuum conditions and intense electron beams used in traditional TEM. The water that surrounds the molecules evaporates, and the high energy electrons burn and destroy the molecules. CryoTEM uses frozen samples, gentler electron beams and sophisticated image processing to overcome these problems. The sample of liposomes used for Cryo-TEM was made of DOPC lipid rehydrated with 80% v/v of milliQ water and 20% v/v EtOH. The fresh sample was then diluted 1/100 in milliQ water before the measurement. All images with Cryo-TEM and TEM were taken at the faculty of biosciences of the Universitat Autònoma de Barcelona (UAB) using a Jeol 2100 electron microscope.

### **3.4 Other Characterization Techniques**

#### **3.4.1 Preliminary Study of Stability**

In order to adapt the solvent exchange procedure to pBAE nanoparticles, where the use of an ethanolic solution is required, a stability experiment was performed to see if they maintain their structure in a solution of EtOH and milliQ water. Lyophilized nanoparticles were rehydrated with the ethanolic solution (evaluated 40% and 20% of EtOH) and characterization measurements with DLS and NTA were made.

Furthermore, since sonication and extrusion were evaluated as optional steps for the purification of lipid nanosystems, additional stability studies were conducted for pBAE nanoparticles. Nanoparticle samples were sonicated in an ultrasonic bath for 30 seconds at a frequency of 40 kHz, then extruded through a syringe filter made of polyvinylidene fluoride (PVDF), with pore size 0.22 and/or 0.45  $\mu\text{m}$ , and subsequently characterized in terms of size, size distribution, and  $\zeta$ -potential.

#### **3.4.2 Confocal Microscopy**

To evaluate the colocalization and interaction between pBAE nanoparticles and liposomes, a fluorescence experiment was performed using confocal microscopy with the instrument Leica TCS SP8 laser-scanning confocal spectra microscope (Leica Microsystems Heidelberg, Mannheim, Germany). The lipid film in the round flask was made by evaporating a volume of DOPC in chloroform with the addition of 1% of the

fluorescent phospholipid (NBD-PE). Fluorescent nanoparticles with Cy5-Cy3 on the other hand were previously prepared as described above and lyophilized, and when necessary rehydrated with the same initial volume of milliQ water. The second encapsulation method was chosen for the experiment, in which the colloidal solution of Cy3-Cy5 nanoparticles is used to rehydrate the fluorescent lipid film.

### **3.5 *In vitro* Cell Transfection Studies**

For the transfection of adherent cell cultures using lipidic nanosystems prepared with pBAEs-pGFP nanoparticles with the second encapsulation method, human lung adenocarcinoma cell line, A549 (ATCC® CCL-185TM), was used as model. A549 were cultured in Duplecco's Modified Eagle's Medium (DMEM, 4.5 g glucose/ml without glutamine, pH=7.2) supplemented with 10% of Fetal bovine serum (FBS), 1% penicillin/streptomycin mixture and the amino acid glutamine. Cells were grown in cell culture dishes (corning) and incubated at 37 °C with 5% CO<sub>2</sub> atmosphere during successive passages. When cells had grown enough to reach the appropriate cell number to get a confluence of approximately 70% for plasmid transfections, cells were seeded on a 96-well plate at a concentration of 10<sup>4</sup> cells/well. Seeded cells were incubated at 37 °C in 5% CO<sub>2</sub> atmosphere for 24 h. After 24 h, the cells were cleaned with PBS (100 µL) and pBAE/nucleic acid nanoparticles were added to the 96-well plate diluted in DMEM at a final concentration of 0.3 µg/well of nucleic acid. To evaluate the transfection level, the cells were incubated for 48 h in a standard CO<sub>2</sub> incubator, washed with PBS, trypsinized with trypsin-EDTA and finally fixed with PFA 4% (25 µL). In the case of the use of pGFP as nucleic acid, the pGFP expression was quantified by flow cytometry (NovoCyte, ACEA Biosciences) and compared against a negative control of untreated cells and a positive control of Lipofectamine® 3000 (Invitrogen by Life technologies, Thermo Fisher Scientific). *In vivo* cell transfection studies were performed for classical KH-nanoparticles, sonicated KH-nanoparticles, lipid-coated nanoparticles (prepared with the second method), and finally sonicated and filtered lipid-coated nanoparticles (prepared with the second method).

## **CHAPTER IV. RESULTS AND DISCUSSION**

## Chapter IV: Results and discussion

### 4.1 Liposomes

As it has been mentioned above, the use of liposome and lipid-based formulations helps to solve problems of cytotoxicity, chemical and colloidal biostability of nanoparticles, also changing their biodistribution or/and favouring the interaction of the latter with target cells.

The physicochemical properties of liposomes, such as surface charge and size, greatly influence their stability. In general, liposomes with very large sizes (diameter greater than 200nm) are cleared from the bloodstream more rapidly than small ones [82]. Several studies, therefore, show that the optimal diameter is around 100 nm [83]. Instead, the presence of charges on the surface promotes the recognition and thus elimination of liposomes from the bloodstream. Negatively charged liposomes have a short half-life compared to neutral liposomes while positively charged liposomes being toxic are quickly removed from the circulation.

In this thesis, neutral lipids such as POPC and DOPC (100% w/w) were chosen to be used for lipid formulations. For the synthesis of empty liposomes, the solvent exchange method was tested, and different samples were prepared with a different amount of organic solvent.

In **Figure 15**, the size distributions and concentrations obtained with the NanoSight are reported. The average diameter is bigger than the one measured with TEM because this is a measure of the light scattering on the single nanoparticles surrounded by its solvation layer while it is moving under Brownian motion.

**Figure 16** reports cryo-TEM images of Liposomes (formulation with 80%20% v/v of milliQ water and EtOH) not purified with sonication and/or filtration and real size distribution obtained by manually analyzing at least 100 nanoparticles, showing particles' diameters between 30 and 100 nm. It is possible to notice above all the presence of multilamellar liposomes and their polydispersity due to the absence of purification steps. In particular, sonication would allow the membranes of MLVs to be broken and unilamellar liposomes to be obtained. Extrusion, on the other hand, which is carried out under pressure from a filter with a specific porosity, would reduce the diameters of the liposomes.

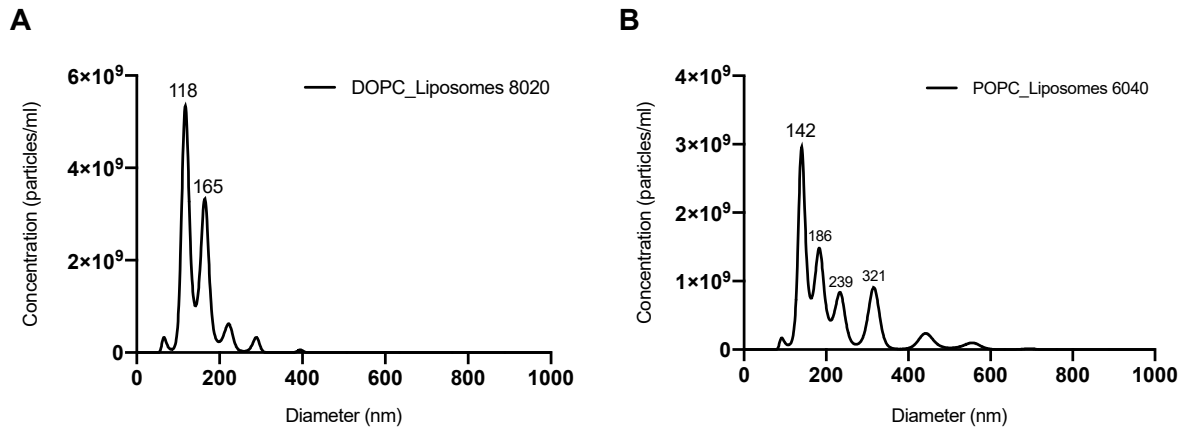


**Figure 15.** Data obtained at NanoSight showing concentration as a function of diameter. A) represent the solution containing DOPC liposomes obtained with 80% v/v milliQ water and 20% v/v EtOH ( $2 \times 10^{11}$  particles/mL) and B) the sample with POPC liposomes with 60% v/v milliQ water and 20% v/v EtOH ( $2.04 \times 10^{11}$  particles/mL).

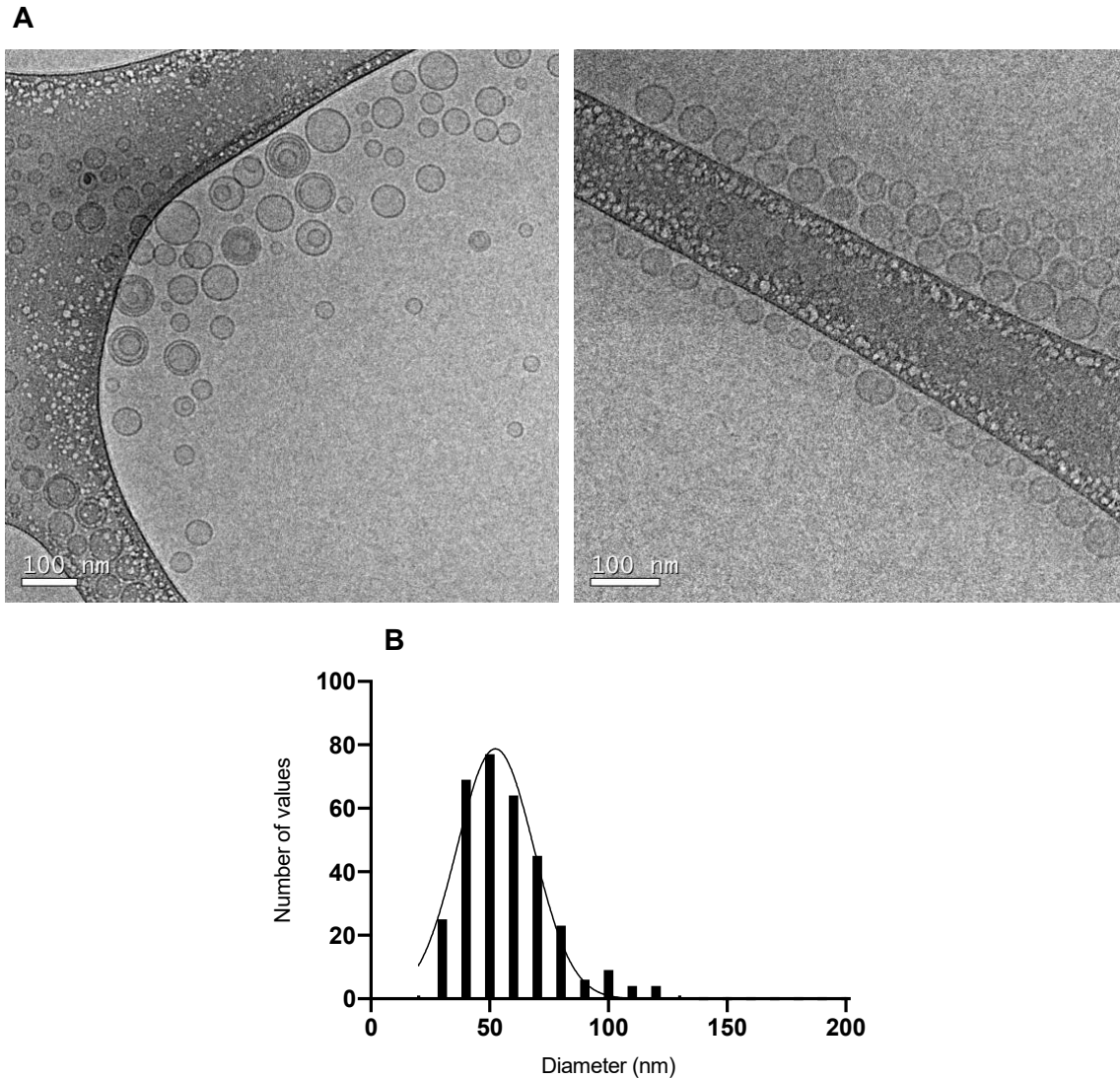


**Figure 16.** A) Cryo-TEM images of Liposomes (formulation with 80%20% v/v of milliQ water and EtOH) showing MLVs and ULLs and B) real size distribution (30-100 nm).

## 4.2 Gold Nanosystems

### 4.2.1 Gold Nanospheres

In **Figure 17** there are the size distributions and concentration obtained by the NanoSight and related to Gold Nanoparticles, stored at room temperature after the synthesis and diluted 1:10 for the analysis, and the real size distribution obtained directly by particle-by-particle analysis from TEM images showing a monodispersity around 15 nm. The diameter of the nanoparticles from NTA is around 48 nm while a second peak at 95 nm shows the presence of larger aggregates. The presence of these aggregates is also confirmed by the images obtained at TEM and shown in **Figure 18**.

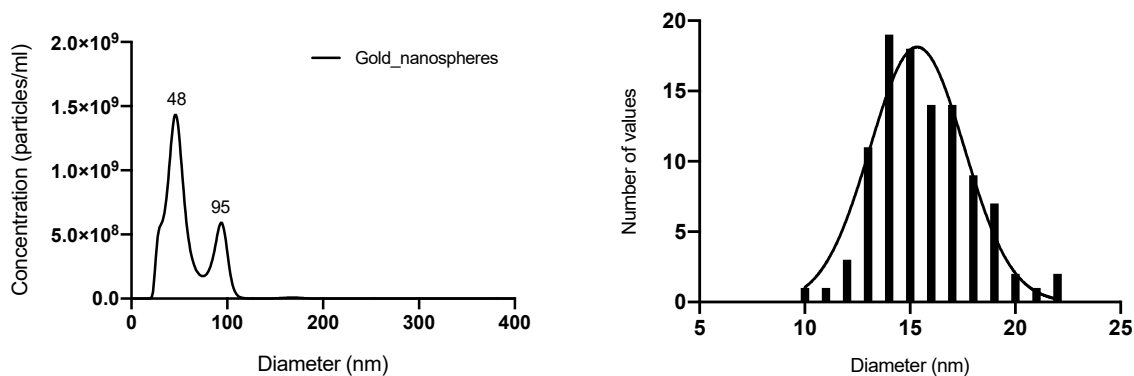


**Figure 17.** Size distribution and concentration ( $4.32 \times 10^{10}$  particles/mL) of Gold Nanoparticles obtained from NanoSight analysis on the left, and real size distribution on the right.

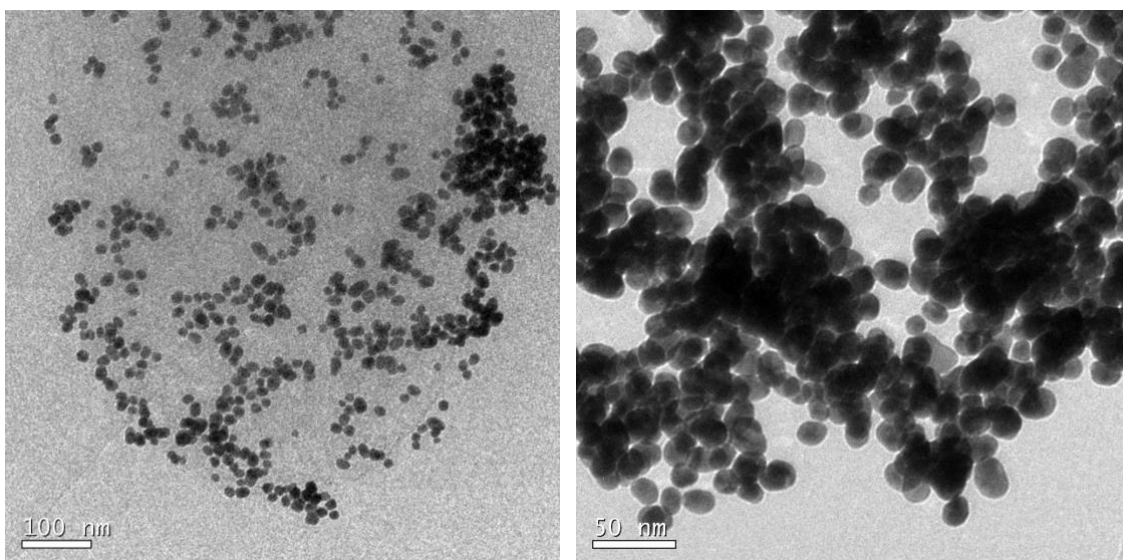


**Figure 18.** TEM images of Gold Nanospheres showing also some aggregates.

The sodium citrate used for the synthesis of gold nanospheres has a dual function: it acts as a reducing agent but, as it adsorbs on the surface, it also acts as a stabilizer, preventing the aggregation of suspended particles. Therefore, by adjusting the amount of sodium citrate, the particle size can be controlled: the more amount of trisodium citrate, the smaller and stable obtained nanoparticles are. This feature is very important for obtaining specific optical characteristics of particles. These properties derive from localized surface plasmon resonance (LSPR), which is also responsible for the color of the Au NPs colloidal solution and is influenced not only by the size, but also by the shape of Au NPs. For small (~10-20 nm) monodisperse gold nanoparticles, the surface plasmon resonance phenomenon causes an absorption of light show around 520 nm and has a red-color solution [56] [84].

In **Figure 19**, we can see the solution obtained from the synthesis of our gold nanoparticles, which confirms the results obtained from the analysis of the TEM images: red colloidal solution and size of nanoparticles between 10 and 30 nm.

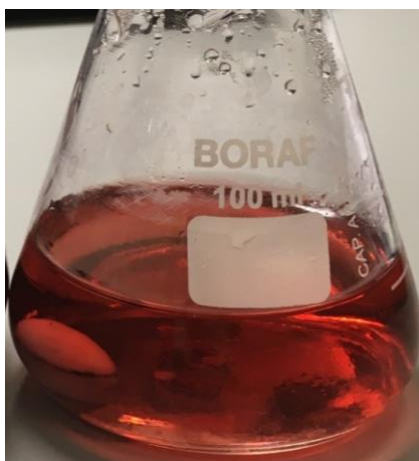


**Figure 19.** Our colloidal solution obtained after synthesis showing red color and therefore confirms what the bibliography states.

#### 4.2.2 Gold Nanorods

Gold Nanorods were synthesized according to the seed-mediated growth method with two steps described before. Size distribution and concentration obtained by the NanoSight are showed in **Figure 20**. From this graph we can see the presence of two main peaks due to the two sizes of rods (around 69 nm and 98 nm).

As in the case of liposomes and gold nanoparticles, the analysis carried out directly from the images obtained at TEM (**Figure 21**) show a distribution of the two dimensions clearly smaller than the NTA graphs. After TEM imaging, sizes were

determined by measuring the length and diameter of nanorods randomly selected. In addition, we can see that the two main components of the sample in TEM images are nanoparticles and nanorods, and that following the washing steps with centrifugation, nanorods have been separated from the spherical nanoparticles.

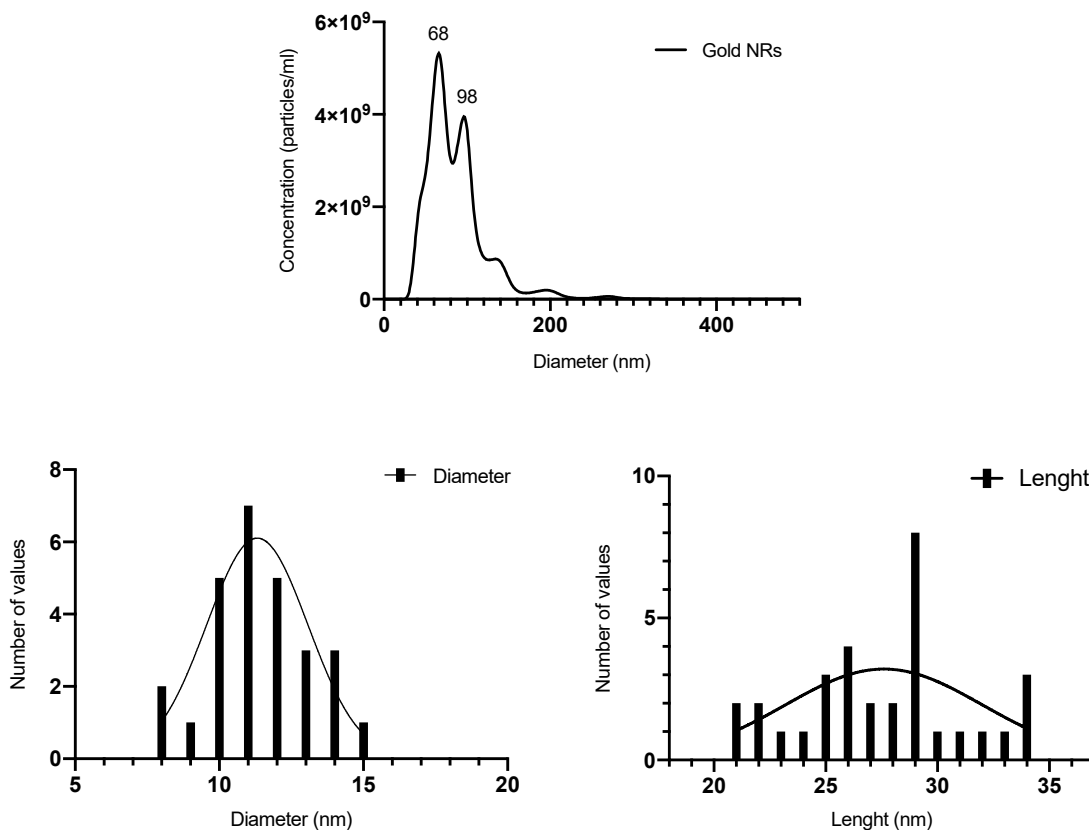


**Figure 20.** On the top, NTA result of diameter and length of AuNRs and concentration ( $3 \times 10^{11}$  particles/mL). On the bottom, sizes determined by measuring the length and diameter of at least 10 rods randomly selected from TEM images, respectively  $\sim 11$  nm e  $\sim 27$  nm.

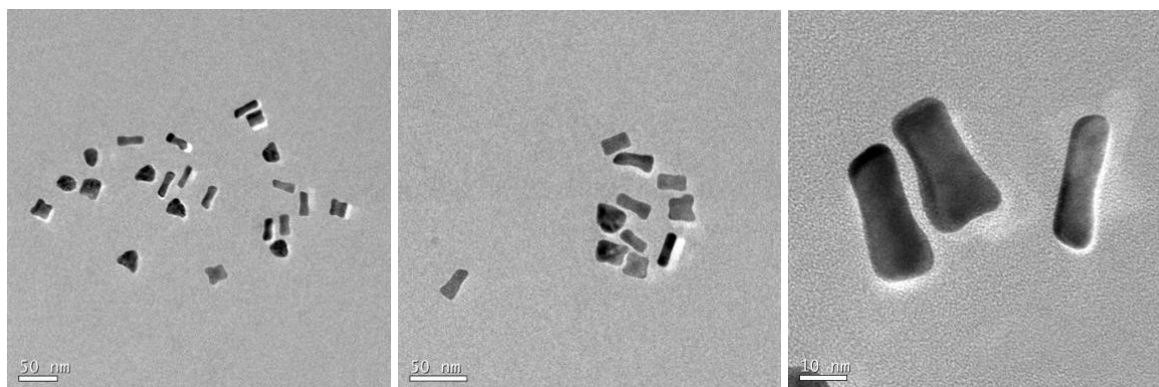


**Figure 21.** TEM images of Gold Nanorods.

As stated above for gold nanoparticles, the size and optical properties of nanorods can also be varied during synthesis. In particular, the aspect ratio (length/width) can be controlled by varying amounts of silver acetate and CTAB. Gold nanorods present two LSPR bands: one is a weak band with a wavelength similar to spherical AuNPs (absorption around 520 nm) due to the plasmon oscillation along the short axis (transversal) and the second is a band in the red-near-infrared (NIR) region due to the plasmon oscillation along the long axis (longitudinal) [56] [58]. Therefore, gold nanorods of different aspect ratios have different sizes and different colour solutions: a light blue solution stands for an AR around 2,4 up to a bright red solution that should have an AR of 5,7 [56].

In **Figure 22**, we can see the dark solution obtained from the synthesis of our gold nanorods, which confirms the results obtained from the analysis of the TEM images: size of nanorods around 27 nm (length), 11 nm (width) and the resulting aspect ratio of approximately 2,5.

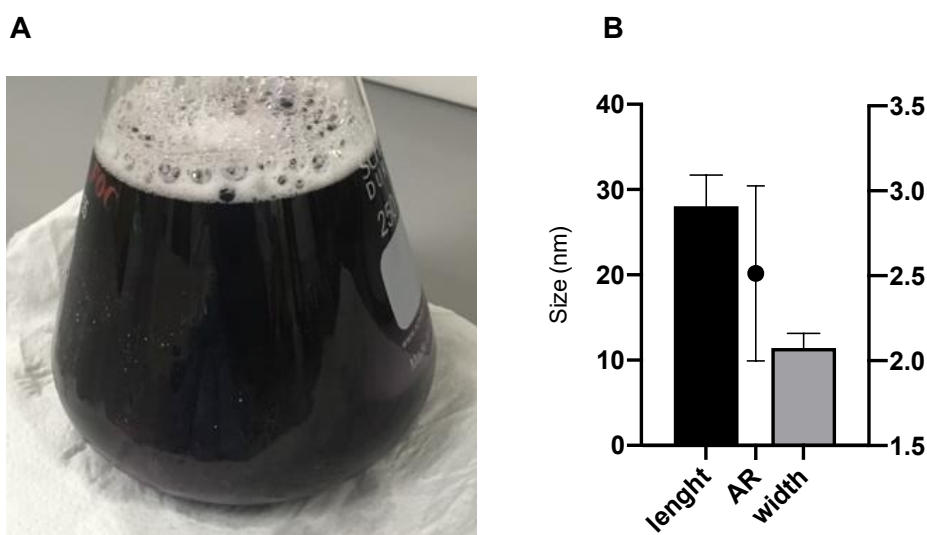


**Figure 22.** A) Our colloidal solution obtained after synthesis showing dark violet color and therefore confirms what the bibliography states. B) Sizes determined by measuring the length and diameter of nanorods randomly selected from TEM images and resulting aspect ratio (length/width).

### 4.3 PBAE Nanoparticles

#### 4.3.1 Previous Studies

To obtain an efficient gene therapy, a well-designed delivery vector is needed. It has been proved before that pBAE is able to encapsulate pDNA/mRNA into discrete nanoparticles and also that the oligopeptide end-modified influences the

complexation efficacy of these nanoparticles [85].

The polymer backbone structure plays a key role in controlling polyplexes behaviours in terms of stability and transfection efficiency, the hydrophobicity can be modified according to the amino radicals, the most common ones are **C32** and **C6** polymers. In further studies, it has been proved that the **C6 pBAE** is the most promising candidate in terms of transfection efficiency/stability [86].

Moreover, another study has shown that the **KH nanoparticle formulation**, which consist of 60% C6CK3 + 40% C6CH3, has suitable characteristics to be administrated intravenously: safe and efficient transfection in different cell lines, even after their lyophilization. While lysine (K)-modified PBAE have demonstrated enhanced interaction to cell membranes, histidine (H)-modified PBAEs are used due to histidine buffering capacity at pH  $\approx$  5–6, which is required for the endosomal escape and penetration to the cytoplasm, where mRNA can be traduced to the protein it codifies for.

Moreover, *in vivo* studies have demonstrated the capability of these nanoparticles to efficiently penetrate and transfect different model cell lines, among them APCs such as macrophages and dendritic cells, after their intravenous administration [18].

With this in mind, nanoparticles composed of KH pBAE (or R as a substitute for K in some cases) were chosen to apply the solvent exchange method so as to improve their stability in a physiological environment and to add in the future targeting moieties to selectively target dendritic cells. In addition, preliminary studies on the stability of these nanoparticles in ethanol and following sonication and filtration have been conducted and the results are reported below.

### 4.3.2 Physicochemical Characterization of NPs

Freshly prepared KH-nanoparticles were characterized by means of size and concentration. The average hydrodynamic diameter obtained from DLS measurements was  $\sim$ 190 nm. Accordingly, when measured by NTA, KH nanoparticles size was similar  $\sim$ 180 nm. Regarding the data obtained, it is remarkable that nanoparticles were low polydisperse samples, since PDIs were around to or lower than 0.3. An example of the results is showed in **Figure 23**.

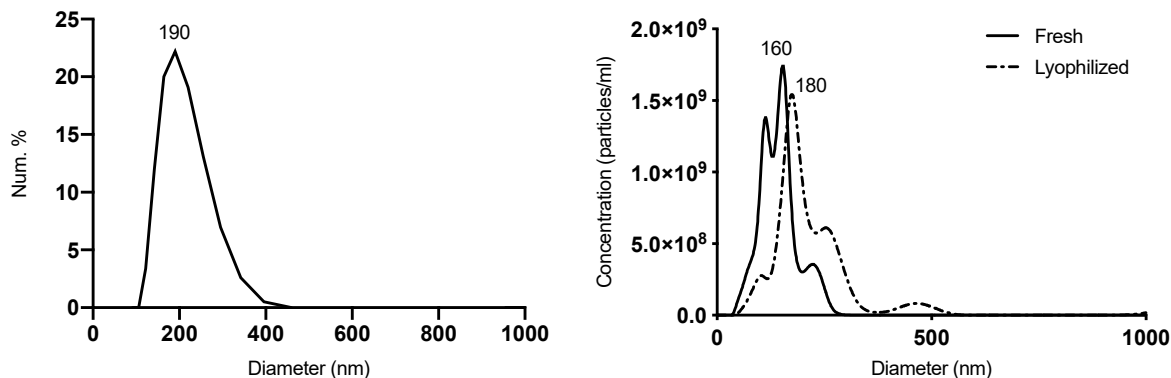


**Figure 23.** Size distribution of fresh KH nanoparticles obtained with DLS on the left. On the right, an example of the NTA hydrodynamic diameter measurement (in nm) of the KH nanoparticles, before and after lyophilization.

After lyophilization, pBAE nanoparticles usually showed a slight size increase (~10–20 nm), while maintaining their low polydispersity, therefore, they can be lyophilized to enable a long-term storage time, in terms of nanoparticle physicochemical properties. These size properties make them adequate for an intravenous administration [18]. Surface charge was also measured to ensure that they were appropriate for intravenous administration. Surface charges were positive (around 24 mV), as expected, due to the presence of cationic oligopeptides at the end termini of the polymers.

In **Figure 24**, there is a cryo-TEM image of a model pBAE nanoparticles, made with 100% of C6CR3 (Cys-Arg-Arg-Arg) polymer as substitute of C6CK3 typically used. With only CR3 polymer and at a doubled weight ratio (pBAE:pGFP, 50:1), nanoparticles are very small in diameter and they have a strongly positive surface charge and therefore they have a low stability after lyophilization, tending to aggregate. On the side is shown the real size distribution obtained by manually analyzing at least 100 nanoparticles, showing particles' diameters between 50 and 150 nm.

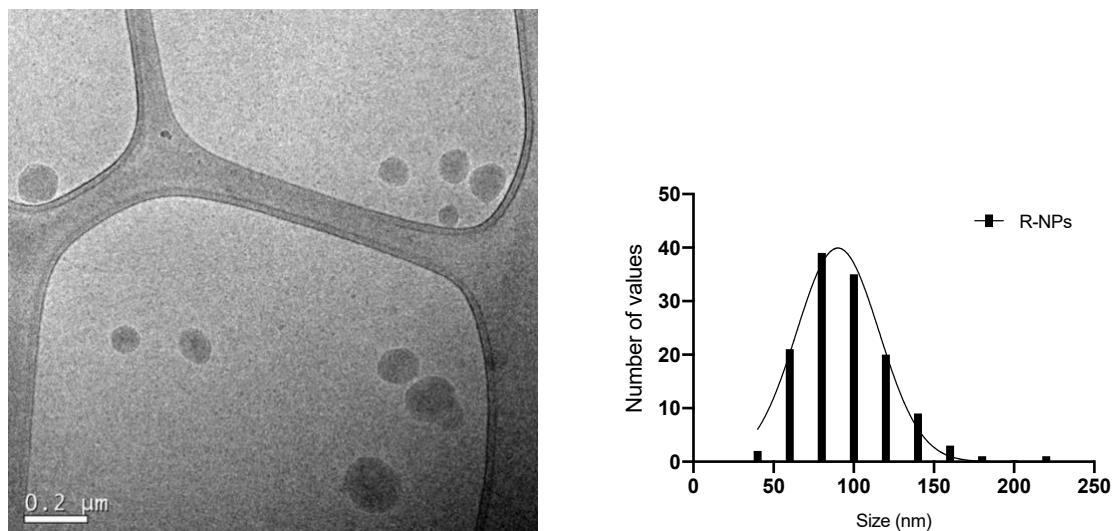


**Figure 24.** Cryo-TEM images of R-Nanoparticles after lyophilization, made with 100% of C6CR3 (Cys-Arg-Arg-Arg) polymer. On the right, real size distribution obtained by manually analyzing nanoparticles' diameter from cryo-TEM images.

### 4.3.3 Preliminary Studies of Stability

- **Ethanol Solution**

Before applying the solvent exchange method to pBAE nanoparticles, further stability studies were conducted, as the method involves the use of a solution containing 40% v/v of ethanol. Lyophilized nanoparticles were resuspended with the solution of 60% v/v milliQ and containing 40% v/v ethanol. Two different formulations of nanoparticles (KH-NPs and R-NPs) were tested for the first step, and for the second three sample replicates of lyophilized KH-NPs were used. Characterization results are shown in **Table 2** and **Figure 25**, below.

**Table 2.** DLS results of stability experiment in a solution with 40% v/v ethanol.

Nanoparticle Formulation	Fresh NPs		Lyophilized NPs 40% EtOH	
	Hydrodynamic Diameter (nm)	PDI	Hydrodynamic Diameter (nm)	PDI
KH-pGFP	263,1	0,2	<b>60,67</b>	0,7
R-pGFP (50:1)	137,7	0,3	<b>4222</b>	0,6

As we can see from the results shown in the table, pBAE-Nanoparticles did not maintain their structure and stability and appeared aggregated or too polydisperse

for the analysis of the hydrodynamic diameter distribution with DLS. Therefore, the test was repeated decreasing the amount of ethanol to a percentage of 20% v/v.

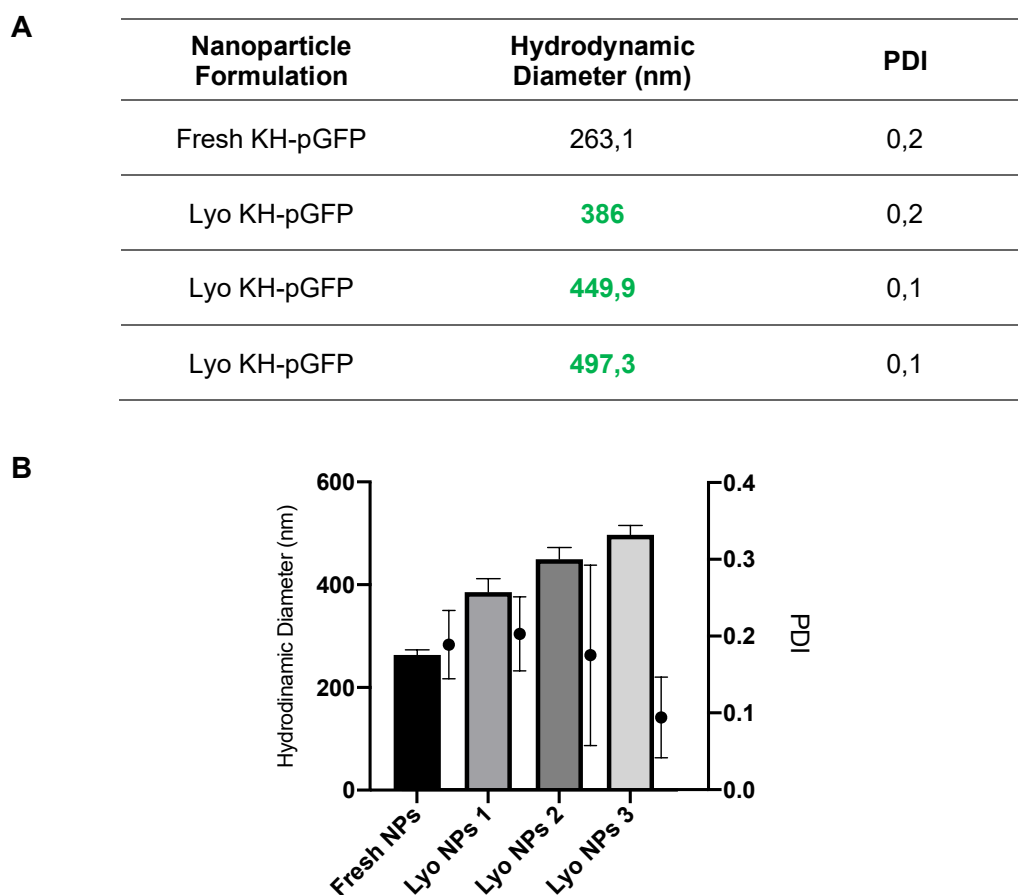


**Figure 25.** DLS results of stability experiment in a solution with 20% v/v ethanol: A) Table with all numerical parameters analysed; B) Hydrodynamic diameter (bars) by DLS of fresh and lyophilized NPs. PDI values are presented in dots, of fresh and lyophilized NPs.

At 20% v/v of EtOH, pBAE-nanoparticles appear to have no change in structure, although their diameter increases considerably compared to the formulation before freeze-drying. However, the data show a low polydispersity given by PDI values that remain in a range between 0.1 and 0.3. it is therefore likely that further studies regarding the stability of pBAE polyplexes in ethanol are required to confirm this theory.

Nevertheless, these results are also confirmed with size distribution analysis with the NanoSight. For this test, nanoparticles with C6CR3 polymer were used. As stated before, with only CR3 polymer, nanoparticles have a strongly positive surface charge and therefore they have a low stability after lyophilization. However, the presence of ethanol does not seem to affect their structure too much (**Figure 26**).

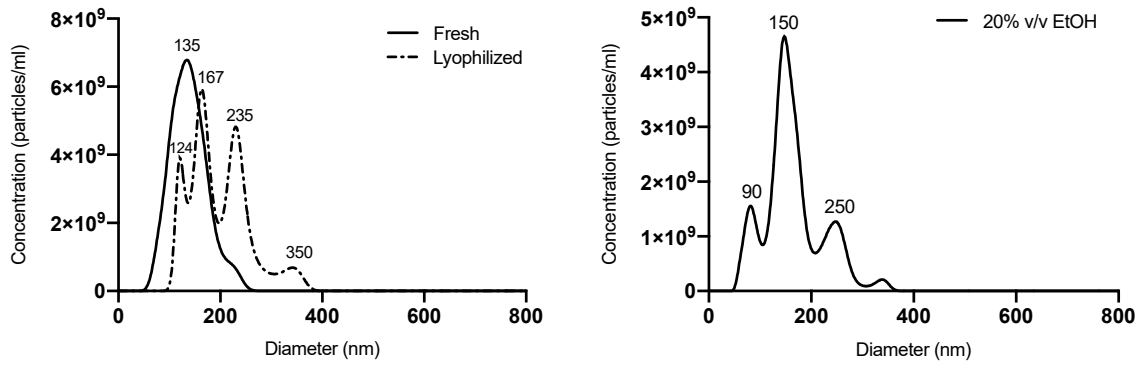


**Figure 26. Effect of ethanol on NPs.** NTA analysis of R-pGFP NPs (50:1) on the left before and after lyophilization. Redispersion of the same nanoparticles with the ethanol solution 20% v/v, on the right graph.

#### • Effect of Sonication on NPs

Sonication (or ultrasonication), along with extrusion through a filter, is a key step in producing monodisperse unilamellar liposomes and controlling their size [87]. In this thesis, sonication and extrusion were evaluated as optional steps for the purification of lipid nanosystems. Therefore, stability studies for pBAE nanoparticles were conducted previously. Samples of nanoparticles were sonicated in an ultrasonication bath for 30 seconds at a frequency of 40 kHz and subsequently characterized in terms of size, size distribution and  $\zeta$ -potential.

**Figure 27** shows results of fresh KH-pGFP NPs before and after sonication, both obtained with DLS and NTA. The size of NPs remains around  $\sim 164$  nm (PDI 0,2 - 0,3) with Zetasizer, therefore, the effect of sonication does not appear to affect nanoparticles. Similar results are obtained with the NanoSight ( $\sim 160$  nm).

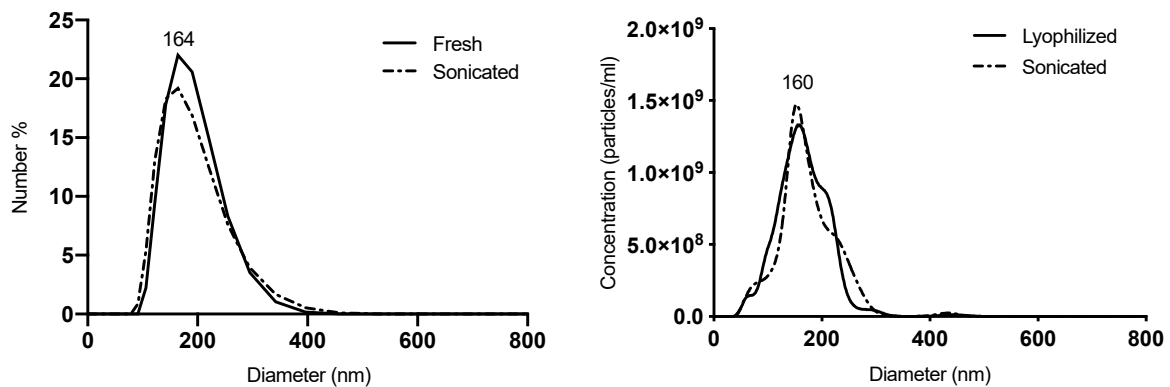


**Figure 27. Effect of sonication on fresh NPs.** DLS analysis of fresh and sonicated KH-pGFP NPs on the left. NTA results of fresh and sonicated KH-pGFP NPs on the right.

**Figure 28**, instead, shows results of lyophilized R-pGFP NPs before and after sonication, both obtained with DLS and NTA. Furthermore, the  $\zeta$ -potential of lyophilized R-NPs (strongly positive in contrast with the KH formulation) was calculated before and after sonication and we can see from the histogram in the figure that it remains in both cases around 42 mV. The size of NPs remains around ~295 nm (PDI 0,4) with Zetasizer, therefore, the effect of sonication does not appear to affect nanoparticles.

Similar results are obtained with the NanoSight (~122-156 nm).

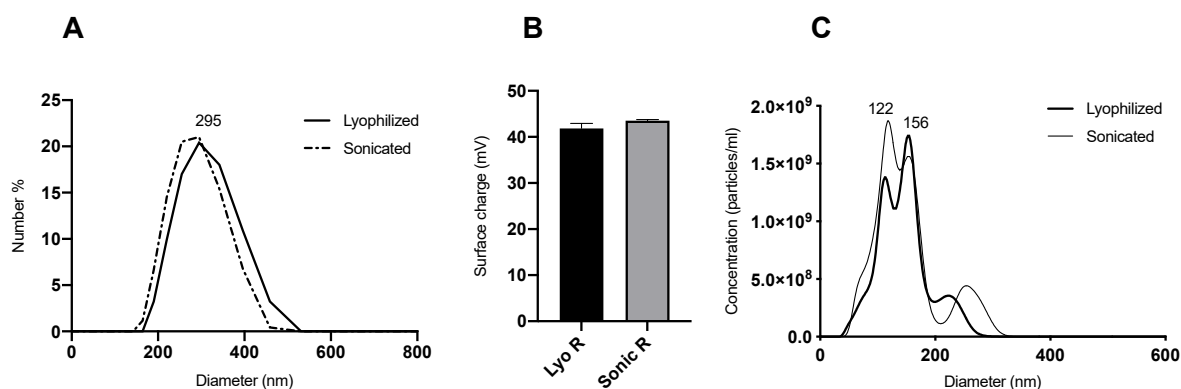


**Figure 28. Effect of sonication on lyophilized NPs.** A) Distribution of hydrodynamic diameter of lyophilized and sonicated R-pGFP NPs. B) Surface charge of lyophilized and sonicated R-NPs. C) Size distribution and concentration by NTA of lyophilized and sonicated R-pGFP NPs.

#### 4.4 Lipid-Coated Nanosystems

Following the protocol previously described for the application of **solvent exchange method**, lipid nanosystems were obtained and the results for both gold nanosystems and pBAE nanoparticles are reported and discussed below.

Briefly, the solvent exchange method has been extensively studied over the years for the controlled deposition of a lipid bilayer on solid substrates. The approach is based on the effects that a solvent, such as ethanol, has on the self-assembly behaviour of lipids. Thus, phospholipids are solvated by alcoholic solvents and exist as monomers at low concentrations of water. However, upon adding water to the solution, lipids begin to self-assemble into liposomes, consisting of a lipid bilayer.

Similar behaviour is observed in the presence of a nanoparticle surface, which provides a favourable support for self-assembly of the lipid bilayer [62].

### 4.4.1 Lipid-Coated Gold Nanospheres

After the application of the solvent exchange method protocol the solution is allowed to equilibrate for some minutes before being characterized. Moreover, for gold nanosystems a physical mixture of metallic particles and liposomes was made to compare their interaction (as they are separated) with respect to their interaction when they are encapsulated.

The results of the size characterisation in relation to concentration with NTA are shown in the **Figure 29**.

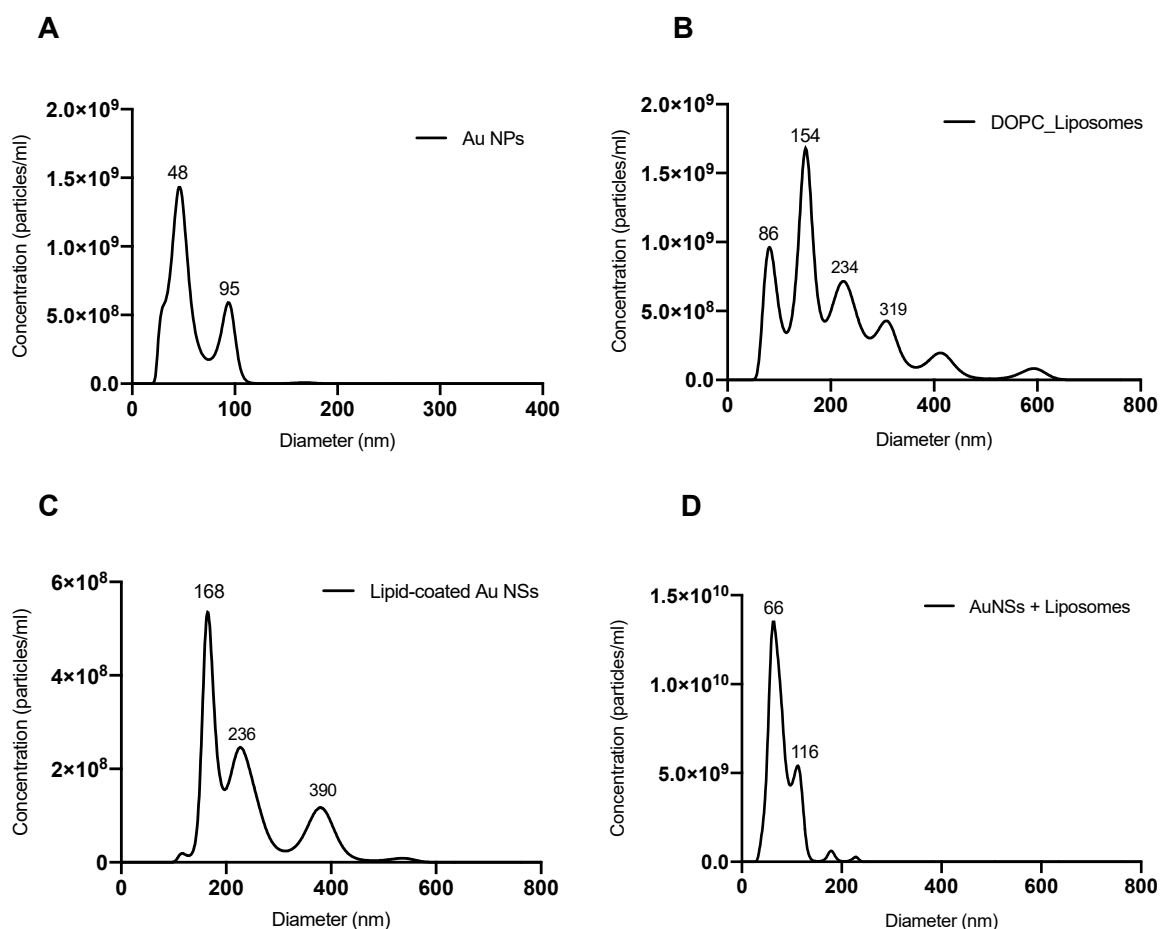


**Figure 29.** Data obtained at NanoSight showing concentration as a function of diameter for A) Au NSs, B) empty DOPC\_liposomes, C) liposomes-coated gold nanospheres and D) the physical mixture of liposomes and AuNSs at 50:50 volume ratio.

In particular, **A** and **B** graphs above compare gold nanoparticles measured after synthesis, without any kind of surface functionalization, which we have already seen in the previous paragraphs, and which mainly have a diameter of around 48 nm measured with NTA, and liposomes, also synthesized using the solvent exchange

method, but that in the absence of purification steps show various sizes between 90 and 300 nm. In **C**, instead, we find the size distribution of liposome-coated gold nanoparticles. We immediately notice the lack of a peak around 40-50 nm, which was present in the graph A, and which could suggest small clusters of AuNSs encapsulated or covered with lipids. The hypothesis that a thin lipid layer was formed around the individual nanoparticles, and that would have increased the size of a few nm [62], should be discarded. It should also be considered that all the AuNPs' samples are in a solution of milliQ water and have a zeta potential around 3.7 mV, thus demonstrating a certain instability and a tendency to aggregate. We could have done a sonication step for few minutes of the AuNPs in water solution to separate the particles and improve their stability before applying the solvent exchange method. Finally, in graph **D** we find the physical mixture of liposomes and nanoparticles in a 50:50 ratio. We can see that the distribution is definitely different from the previous graph and shows a main peak around 66 nm at a high concentration and small peaks at larger sizes. This maybe due to a higher concentration of gold nanoparticles as opposed to liposomes.

Results by cryo-TEM are shown in **Figure 30**.

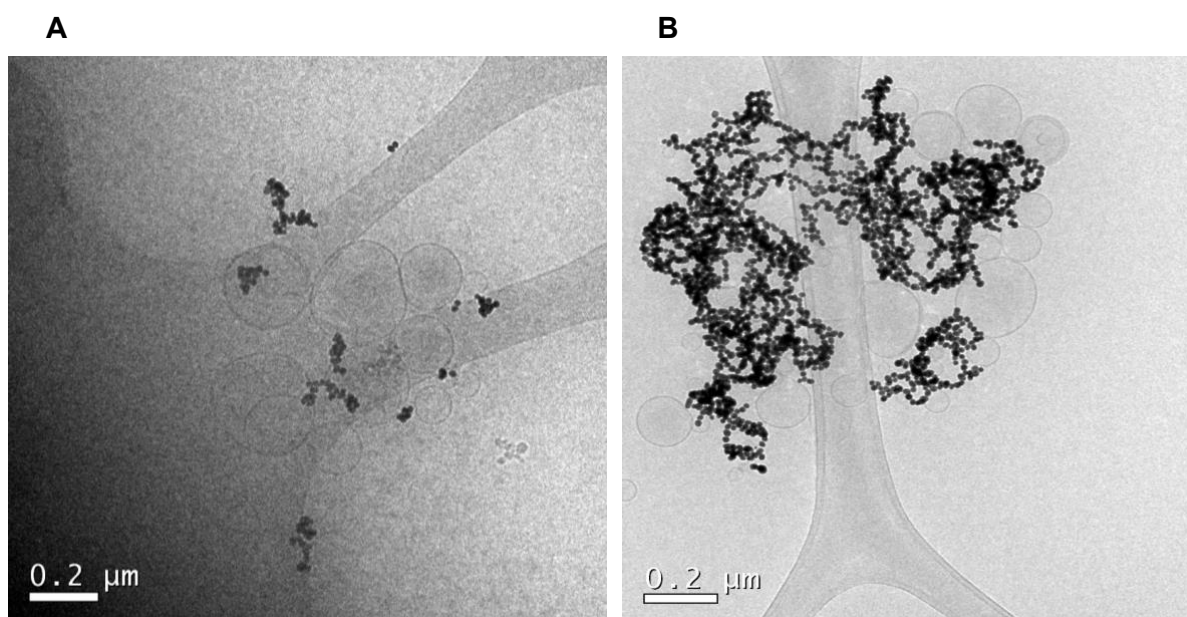


**Figure 30.** Cryo-TEM images of A) lipid-coated Au Nanospheres and B) physical mixture of liposomes and AuNSs at 50:50 volume ratio.

In the image **A** we can confirm the formation of small separate clusters of gold nanoparticles interacting with liposomes both internally and externally. However, we can note the presence of many empty liposomes, this indicates an excess of lipids

that instead in the literature was minimized by applying a step of centrifugation, resuspension in a smaller volume of water and complete cell culture medium (50:50 vol ratio) and moreover the solution was sonicated for a few minutes and filtered to minimize aggregation [63]. In image **B**, regarding the physical mix, it is clear the presence at a higher concentration of gold nanoparticles as opposed to liposomes, and they have a size of about 10-20 nm and tend to aggregate with each other. Liposomes instead have a diameter between 100 and 200 nm, as expected, and do not have clusters of nanoparticles inside them.

#### 4.4.2 Lipid-Coated Gold Nanorods

Exactly the same protocol described for gold nanoparticles was applied for gold nanorods (Au NRs) and the results by NTA are shown in **Figure 31**.

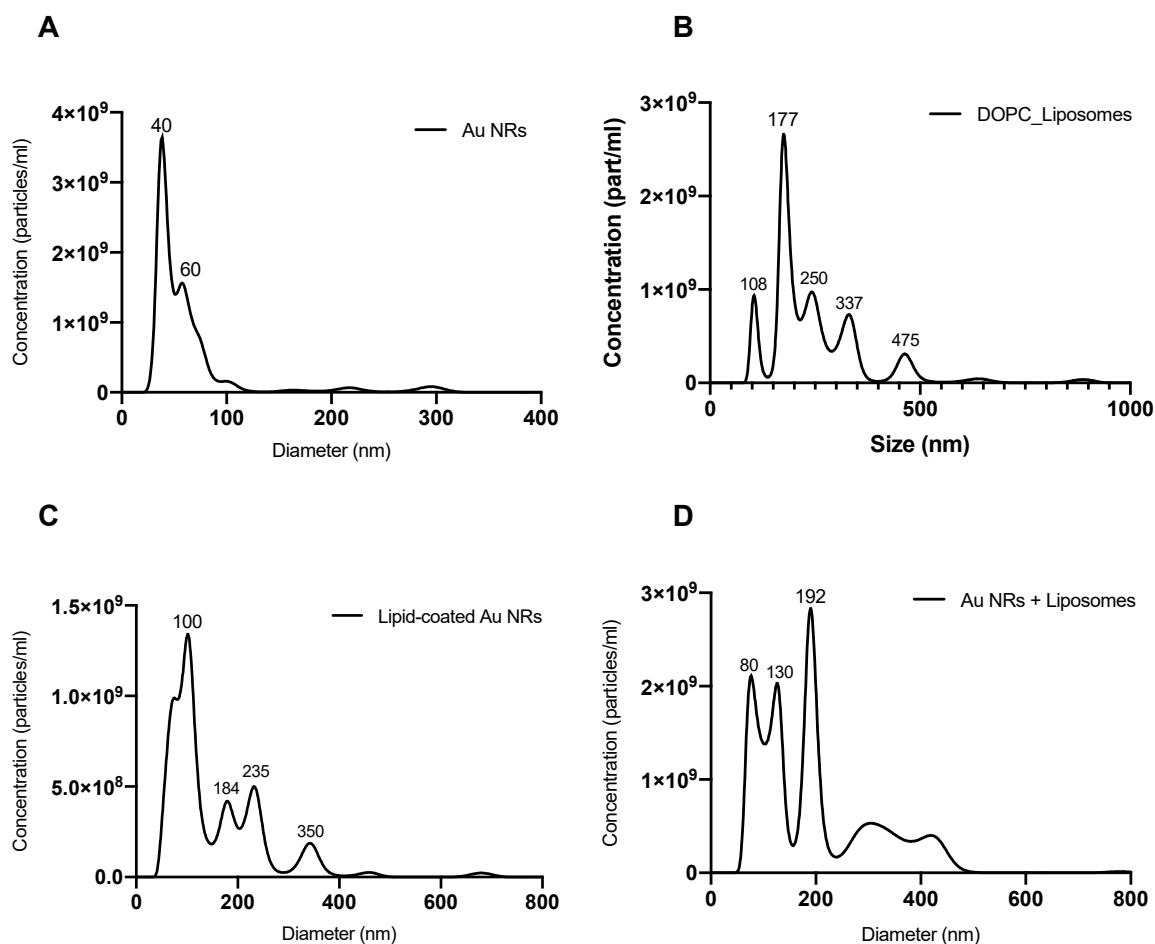


**Figure 31.** Data obtained at NanoSight showing concentration as a function of diameter for A) Au Nanorods, B) empty DOPC\_liposomes, C) liposomes-coated gold nanorods and D) the physical mixture of liposomes and AuNRs at 50:50 volume ratio.

Graphs **A** and **B** show, respectively, sizes in relation to the concentration of the nanorods (40 nm in diameter and 60 nm in length) and of the empty liposomes obtained with DOPC phospholipids, which show a clear polydispersity and varying diameters between 100 and 400 nm. Images **C** and **D**, on the other hand, show similar results with gold nanoparticles. In **C**, we find a main peak around 100 nm showing the formation of clusters of nanorods, and we no longer find the two peaks related to the two dimensions of diameter and length of the nanorods, which instead we can see in the physical mix plot. Again, we cannot confirm the formation of a lipid substrate on the surface of the nanorods. Regarding peaks related to diameters higher than 200 nm they can be removed thanks to sonication and filtration steps. The results described above are also confirmed by the cryo-TEM images below (**Figure 32**).

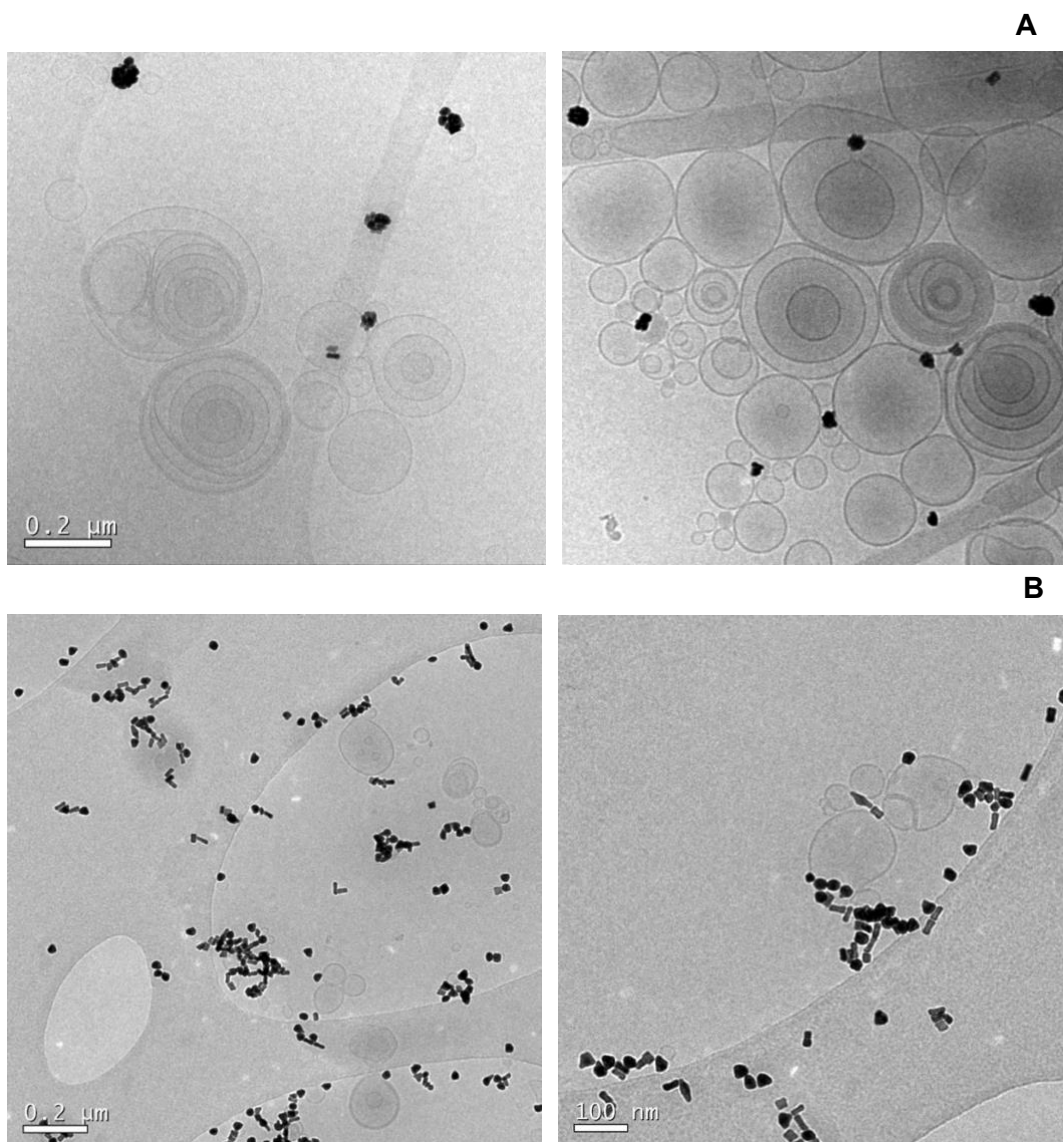


**Figure 32.** Cryo-TEM images of A) lipid-coated Au Nanorods and B) physical mixture of liposomes and AuNRs at 50:50 volume ratio.

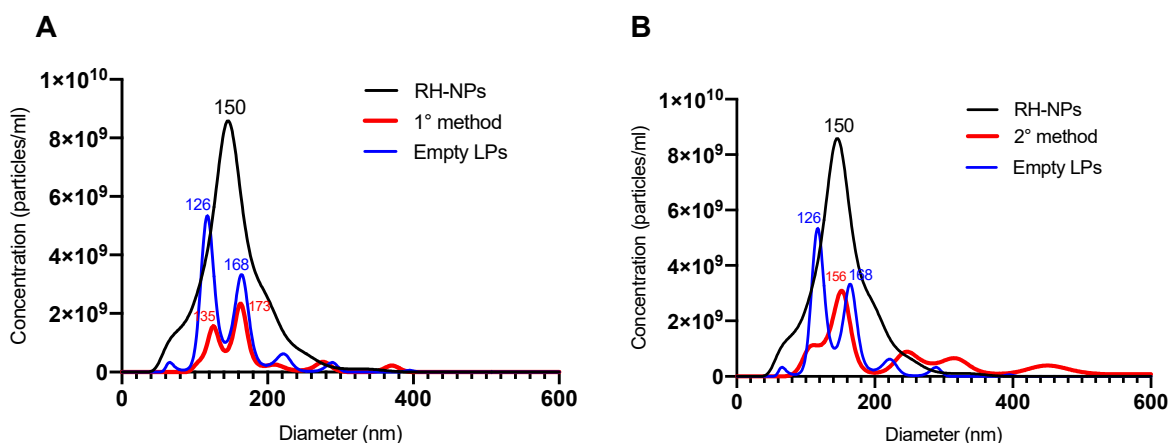
### 4.4.3 Lipid-Coated pBAE Nanoparticles

For pBAE nanoparticles, two different methods of encapsulation in liposomes were developed and evaluated, as a variation of the solvent exchange method because the centrifugation step cannot be applied to pBAE nanoparticles that being formed by electrostatic interactions, with the centrifugal force they would collapse. Protocols are described in previous chapter.

However, we have samples of freeze-dried nanoparticles that in previous studies have been shown to remain stable over time after lyophilization, stored for at least 6 months, at  $-20\text{ }^{\circ}\text{C}$  [22]. In addition, the preliminary study of stability in ethanol showed some stability with an amount of 20%v/v of ethanol, so in the **first method** implemented, the freeze-dried samples were resuspended with a lipid solution containing water and ethanol at a volume ratio of 80:20. Then, the addition of water should be result in the formation of a supported lipid bilayer on the surface of NPs or in an interaction between them and liposomes.

The **second method**, instead, does not involve the use of ethanol as the lyophilized nanoparticles were resuspended with only milliQ water and this colloidal solution used to rehydrate the lipid film of DOPC.

Results are shown in **Figure 33**. RH-NPs formulation was used for NTA characterization and for both encapsulation methods. The same particles were also used for cryo-TEM images.



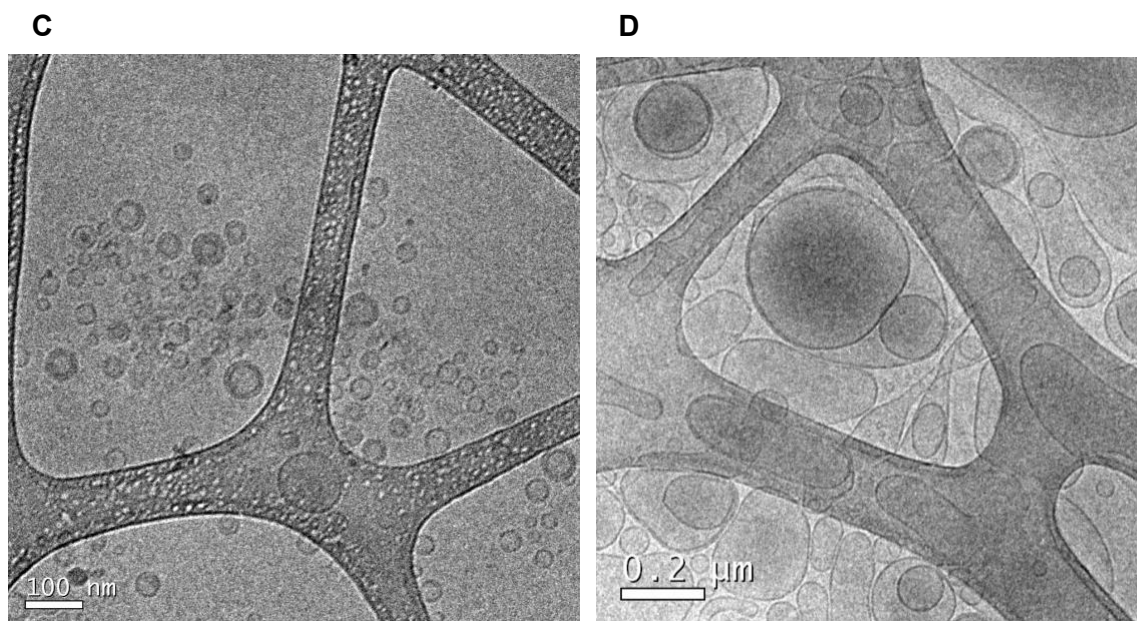


**Figure 33. Characterization of lipid-coated pBAE NPs.** A) B) Data obtained at NanoSight showing concentration as a function of diameter for nude RH-NPs compared with the same formulation but lipid-coated with first and second method and empty DOPC liposomes, respectively. C) D) Cryo-TEM images of first and second encapsulation method, respectively.

As we can see from graphs **A** and **B**, the results obtained from NTA analysis would seem to indicate that the nanoparticles are coated with a lipid bilayer, because in both methods slightly larger peaks appear than in the graph of RH-nanoparticles simply resuspended in milliQ water after freeze-drying. However, looking at the images obtained at cryo-TEM it is very difficult to reach such a conclusion. First of all, it is clear that the absence of ethanol in the second formulation (**Figure 33D**) produces worse liposomes, much larger than usual, not perfectly spherical and especially not separated from each other, moreover it is impossible to recognize the polymeric nanoparticles.

Regarding the first method, instead, from the cryo-TEM image (**Figure 33C**) we note that the presence of ethanol is essential for the formation of liposomes well separated from each other, monodisperse and small in diameter, but even here it is impossible to recognize the polymeric nanoparticles mainly due to the low contrast unlike gold nanoparticles, which instead are more electron-dense and well visible between liposomes.

However, considering the results obtained from the stability experiments in ethanol and also the significant increase in the nanoparticles' size obtained, especially for cell transfection studies we chose to continue the investigation using only **the second**

**method** (without the use of the organic solvent) which produces liposomes of larger size but by adding the **purification steps** the size should reduce significantly. They include: a few seconds of immersion in an ultrasonic bath at 40kHz and filtration with a syringe filter made of polyvinylidene fluoride (PVDF), with pore size 0.22 and/or 0.45  $\mu\text{m}$ .

The results of a purification experiment conducted on nanoparticles composed of 100%v C6CR3 polymer are reported below (**Figure 34**).

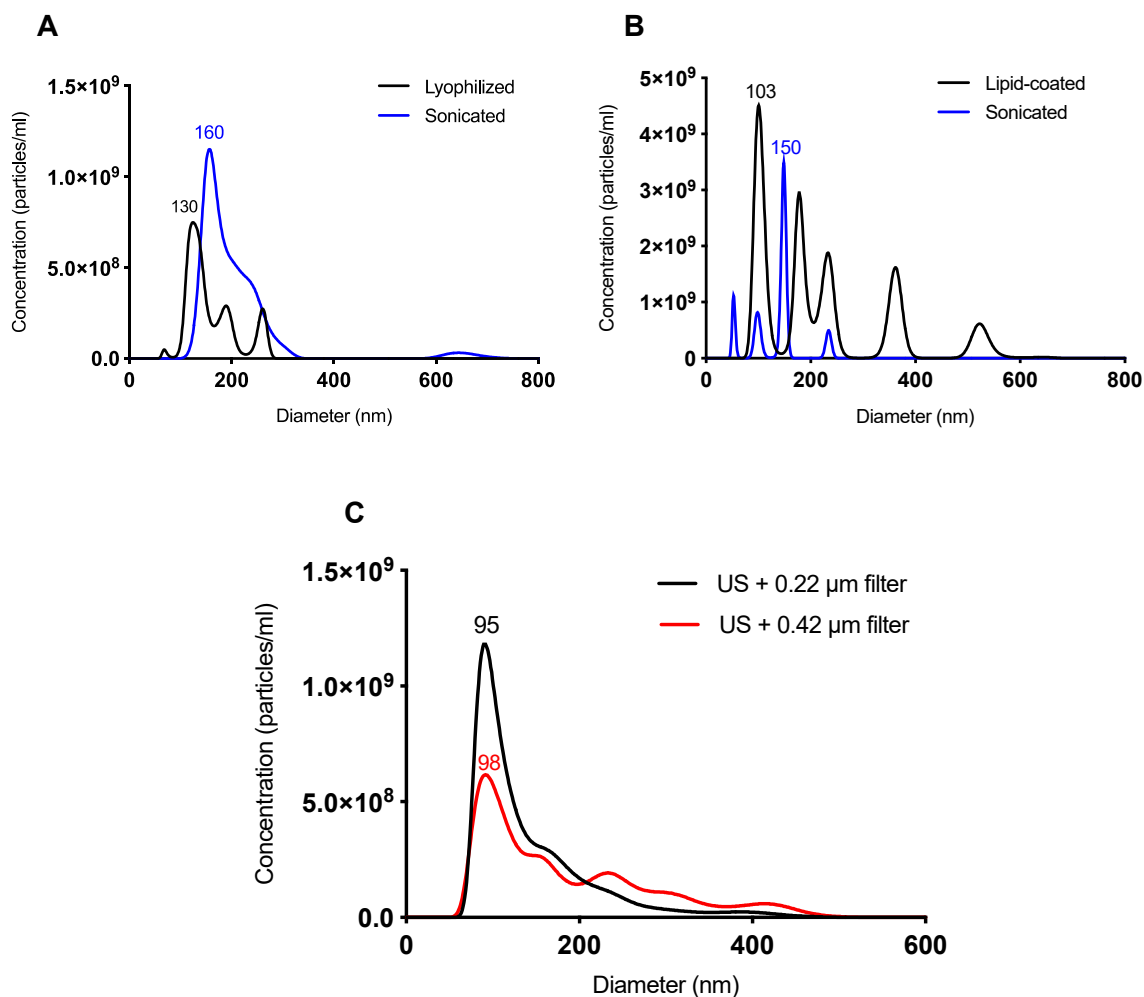


**Figure 34.** Size distribution and concentrations of purified lipid-nanosystems composed of R-NPs obtained with NanoSight. A) Nude lyophilized R-NPs compared to sonicated R-NPs. B) R-nanoparticles encapsulated using the second methodology compared to same nanosystems but ultrasonicated. C) Sonicated and filtered Lipid-nanosystems with different filter size, 0.22/0.45  $\mu\text{m}$ .

In graph **A** we find the size distributions of RH-nanoparticles measured after freeze-drying (in blue) and the same sample after the step in the ultrasonication bath (in black). As we had already seen above, nanoparticles maintain more or less the same distribution; we can see that the larger size peaks in the black graph seem to

decrease and move towards a single peak around 160 nm.

In Graph **B**, instead, the two distributions refer to the lipid nanosystems formed by the second encapsulation method and using a replicate of the RH-nanoparticle sample after freeze-drying. In black we find the distribution of non-sonicated lipid nanosystems and in blue the sonicated ones. In both graphs, the systems are very polydisperse and they have a main peak, around 100 nm and 150 nm for the non-sonicated and sonicated systems, respectively. Although after sonication the main peak increases moving towards 150 nm, we can see that the spikes above 250 nm disappear. We know that sonication, along with filtration, is a mechanical process that allows to reduce the size of vesicles, but more importantly it should allow the formation of a monodisperse solution by breaking down the membranes of multivesicular liposomes and this seems to happen.

Finally, in plot **C**, we find the distributions of the previously described nanosystems extruded through filters with pore sizes 0.22  $\mu\text{m}$  (in black) and 0.45  $\mu\text{m}$  (in red). The sizes in relation to concentrations, are much improved and well monodisperse, with very small diameter around 95-100 nm. Moreover, we can see that the concentration decreases considerably, this confirms that the particle aggregates remain trapped in the filter and only smaller diameter particles are extruded.

These results will be better illustrated by the fluorescence experiment.

## 4.5 Fluorescence Colocalization Experiments

To evaluate the colocalization and interaction between pBAE nanoparticles and liposomes, a fluorescence experiment was performed using confocal microscopy. Fluorescent pBAE NPs were synthesized using labelled polymer with Cy5 dye (red) and labelled pGFP with Cy3 (blue). Instead, lipids were labelled with NBD-PE (yellow). The experiment was conducted on particles encapsulated with the second method both before and after the purification steps in order to compare the effects.

The results are shown in **Figure 35**; row **A** represents nanosystems non-sonicated, and rows **B** two different samples after sonication. First of all, the entire figure shows that the diameter of the vesicles is greatly reduced in the sonication phase and the concentration of very small particles increases.

Regarding the co-localization, in the **merges** column we find in orange the overlapping of lipids and polymer in greater quantity, but we can also notice (in purple) the sporadic presence of non-encapsulated pBAE nanoparticles, especially in the two sonicated samples. While, on the other hand, the very clear and bright spots, tending

to white colour, should represent the total co-localization of polymer, plasmid and lipids.

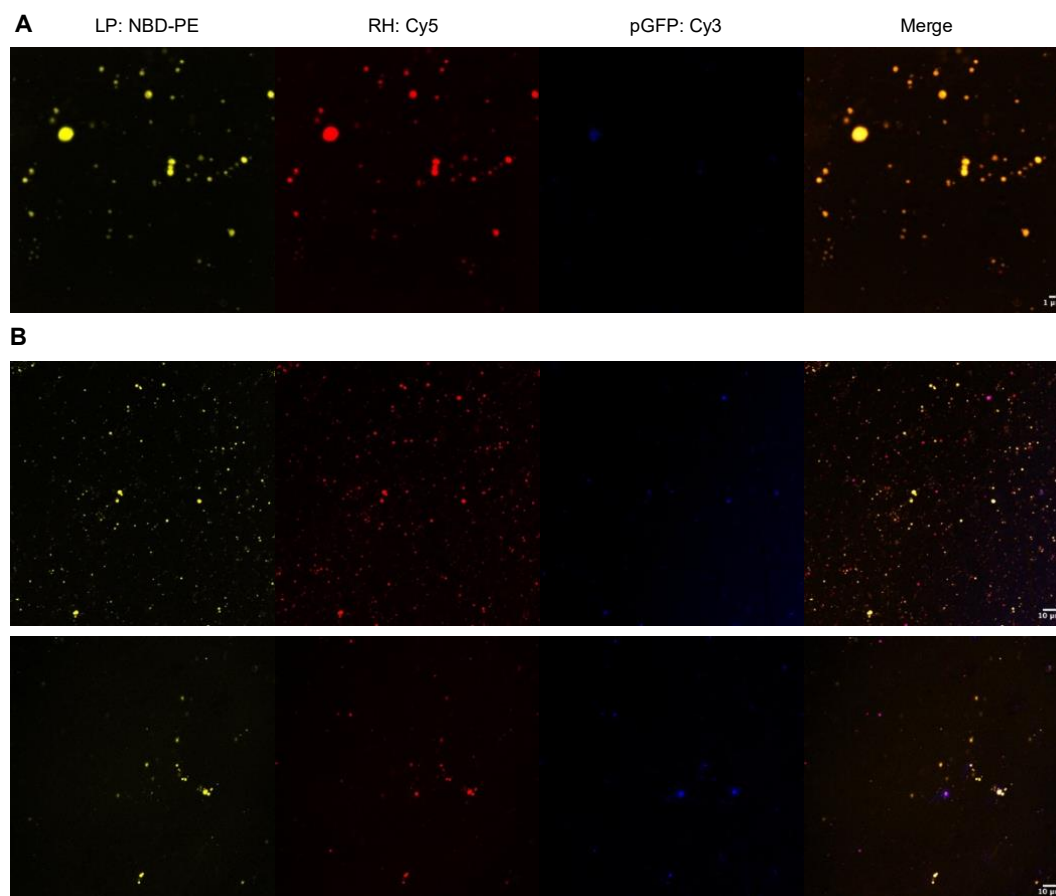


**Figure 35.** Fluorescence image of the (a) liposomes/lipid coating labeled by 1% NBD-PE ( $\lambda_{exc}= 463$  nm); (b) RH-NPs labeled by 1% of Cy5 ( $\lambda_{exc}= 650$  nm); (c) pGFP labeled with 1% of Cy3  $\lambda_{exc}= 550$  nm); (d) the merged channels showing co-localization. Scale bar: 1  $\mu m$ .

#### 4.6 *In vitro* Cell Transfection

After choosing the second method of encapsulation of pBAE-NPs for the reasons previously explained, applying the subsequent steps of sonication and filtration (0.22  $\mu m$  filter was chosen to obtain smaller particles required for cell transfection), and confirming colocalization with the confocal microscope, their effect on transfection efficiency was studied. To accomplish this, all experiments were performed in A549 cells using the pGFP plasmid. pGFP expression was determined by flow cytometry analysis at 48 hours post-transfection. Flow cytometry results are presented in **Figure 36**.

The objective of this study was to test the transfection ability of the lipid nanosystems developed, containing pBAE/pDNA complexes, in contrast to naked KH-formulated nanoparticles (which have already demonstrated their high transfection efficiency in

previous studies) before and after sonication.

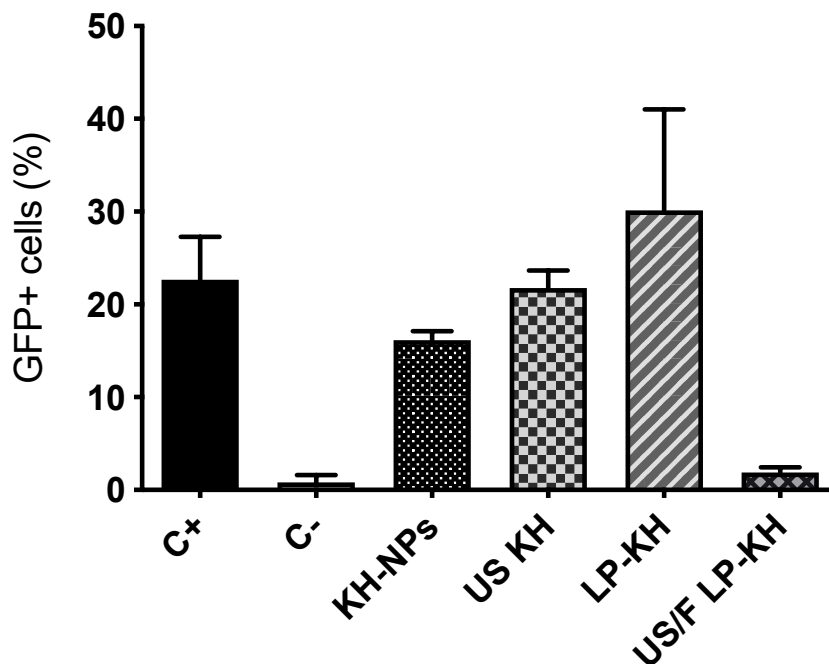


**Figure 35. Transfection efficiency of lipid nanosystems and pBAE polyplexes.**

The studies were done in A549 cell lines. GFP expression was determined by flow cytometry after 48h of the nanoparticle's transfection. Each bar represents the mean  $\pm$  SD. C-, the group without any treatment. C+ lipofectamine.

Looking at the graph above, we immediately notice that, surprisingly, sonicated KH-nanoparticles showed an increase in transfection efficiency compared to non-sonicated KH complexes. Secondly, we can see that the lipid nanosystems showed contrasting results. Lipid-coated complexes without the purification steps showed a very high transfection efficiency but also with a high standard deviation. However, inexplicably, when such systems are sonicated and extruded through the filter, thus eliminating polydispersity and reducing size, the transfection rate decreases sharply towards zero, probably due to the marked decrease in particle concentration already shown as a result of the NTA analyses, and therefore probably a net amount of plasmid remained captured by the filter.

Unfortunately, due to the Covid-19 situation some experiments were not possible to be carried out, including further studies on efficacy of cell transfection to confirm the validity of these results.

## **CHAPTER V. CONCLUSIONS**

## Chapter V: Conclusions

In the last decade, bio-nanotechnologies have brought great improvements to medicine against cancer, developing new biomaterials and therapeutic techniques that are more efficient, patient-specific and have fewer side effects than conventional methods. Among the latter, cancer immunotherapy is gaining attraction, and it is a type of treatment that stimulates the immune system to attack and destroy cancer cells. A particular form of immunotherapy is represented by therapeutic anti-cancer vaccines that directly *in vivo*-transfect antigen-presenting cells (APCs) to stimulate the immune system.

To this end, nanomaterials, in recent years, have shown promising results as vectors for gene delivery, due to their limited size (< 200 nm) allowing them to interact directly with cells at the same scale as most biological properties. In addition, thanks to their intrinsic chemical and physical properties, they allow therapies and diagnostics to be combined in a single nanosystem.

Among the non-viral vectors for gene delivery, the most studied are definitely **gold nanosystems**, of various shapes and sizes, **polymeric nanoparticles** and **liposomes**. The latter were among the first to be approved by the FDA as carriers of against cancer molecules due to their strong biocompatibility and biodegradability and especially versatility for various applications, nevertheless they present limited control of drugs/gene release.

For this purpose, instead, polymeric nanoparticles composed of **oligopeptide end-modified poly ( $\beta$ -aminoester) (OM-pBAE)**, a class of polymer that has easily biodegradable ester bonds, have been developed for their high buffering and gene release capacity once internalized in the cells. However, one of the main problems related to polyplexes is their limited stability, which can be strongly compromised in the presence of ions. To overcome this disadvantage, in this thesis a methodology has been investigated to allow the encapsulation of polymeric or metallic nanoparticles within liposomes or to create a lipid coating with the aim to increase the cell penetration efficiency and biostability.

- As a method of **synthesis of liposomes** or lipid coating was chosen to follow the **Solvent exchange method**, based on the slow removal of the organic solvent from the solution containing lipids through the increase of the amount of water. Preliminarily, therefore, liposomes of size between 30 and 100 nm were

synthesized, although were obtained very polydisperse and multilamellar liposome solutions due to the lack of sonication and/or filtrations steps.

- Subsequently, **gold nanoparticles** of about 20 nm diameter and **gold nanorods** of about 30 nm length and 10 nm diameter were synthesized. In addition to their important physical and optical properties, these metal nanosystems were used to test encapsulation and interaction with liposomes as stable and inert systems unlike pBAE nanoparticles.
- NTA results showed a clear increase in size when particles should have been covered by lipid and the absence of peaks around the diameter of the Au NPs, on the other hand, cryo-TEM images showed the formation of **well-defined clusters of gold particles** but also the excessive presence of empty liposomes, showing how a purification step to remove lipids in excess is necessary. However, the presence of a lipid coating cannot be fully confirmed, and further investigations of the optimal coupling concentration are probably required.
- Regarding pBAE-NPs, in particular formulations containing pBAE modified with lysine/arginine and histidine were used. Preliminary **studies of stability in ethanol** (required in the lipid bilayer coating protocol) and **stability after sonication** were conducted. Although the latter showed positive results, both in terms of size and surface charge, the same cannot be said for stability in ethanol. Two different amounts of ethanol were tested, 40%v and 20%v, and in both cases particles' size changed. However, with 20% ethanol they appeared to maintain their complexed structure with pGFP and their monodispersity, although with a diameter greater than 300 nm.
- The **coupling of liposomes and pBAE nanoparticles** was developed from solvent exchange method but with variations, and thus two different synthesis protocols were obtained. In particular in the second method the use of ethanol has been completely eliminated.
- Although the results of the lipid nanosystems obtained from the NTA analysis show slightly larger peaks than the bare nanoparticles suggesting coupling, cryo-TEM images could not confirm this result, as it was difficult to recognise the polymeric particles. However, further **sonication and filtration steps** were introduced in order to obtain smaller, monodisperse systems and to eliminate any aggregates, and NTA analysis positively confirmed the results, albeit with a marked decrease in concentration.
- The positive effect of sonication was also confirmed in the fluorescence

experiment, which showed a **colocalization between liposomes, polymers and pGFP**, as well as significantly smaller nanoparticles than the non-sonicated system, which on the other hand, showed aggregates of around one micron in size.

In conclusion, some ***in vitro* cell transfection** studies were carried out on adherent cells with sonicated nanoparticles and lipid nanosystems obtained with the second coupling method. Surprisingly, a high transfection efficiency was found for sonicated nanoparticles and lipid-coupled nanosystems, whereas when the lipid nanosystems were sonicated and filtered, the transfection efficiency decreased drastically. This result was probably due to filtration, which retained a high concentration of pGFP in the pores of the filters, decreasing the transfection efficiency.

## **CHAPTER VI. BIBLIOGRAPHY**

## Chapter VI: Bibliography

- [1] H. F. A. E. Naveed Ahmed, "Theranostic applications of nanoparticles in cancer," *Drug Discovery Today*, vol. 17, no. 17-18, pp. 928-934, 2012.
- [2] R. S. A. T. Samer Tohme, "Surgery for Cancer: A Trigger for Metastases," *Cancer Research*, vol. 77, no. 7, p. 1548–1552, 2017.
- [3] S. G. C. L. Junjie Li, "Research perspectives: gold nanoparticles in cancer theranostics," *Quant Imaging Med Surg*, vol. 3, no. 6, pp. 284-291, 2013.
- [4] A. F. M. E Pérez Herrero, "Advanced targeted therapies in cancer: Drug nanocarriers, the future of chemotherapy," *Eur J Pharm Biopharm*, vol. 93, p. 52–79, 2015.
- [5] K. K. N. P. P. W. Meghan Sullivan, "Harnessing the immune system's arsenal: producing human monoclonal antibodies for therapeutics and investigating immune responses," *F1000 Biol Rep*, vol. 3, no. 17, 2011.
- [6] Q. X. A. S. Emily Jen, "FDA Approval: Blinatumomab for Patients with B-cell Precursor Acute Lymphoblastic Leukemia in Morphologic Remission with Minimal Residual Disease," *Clinical Cancer Research*, vol. 25, no. 2, pp. 473-477, 2019.
- [7] B. M. K. S. Khoja L, "Pembrolizumab," *Journal for ImmunoTherapy of Cancer*, vol. 3, no. 36, 18 August 2015.
- [8] M. A. Stanley Oiseth, "Cancer immunotherapy: a brief review of the history, possibilities, and challenges ahead," *J Cancer Metastasis Treat*, vol. 3, pp. 250-261, 2017.
- [9] W. G. P. C. Cameron F, "Ipilimumab: first global approval," *Drugs*, vol. 71, no. 8, p. 1093–1104, 2011.
- [10] B. I. L. A. S. P. B. F. C. R. Lynch TJ, "Ipilimumab in combination with paclitaxel and carboplatin as first-line treatment in stage IIIB/IV non-small-cell lung cancer: results from a randomized, double-blind, multicenter phase II study," *Journal of Clinical Oncology*, vol. 30, no. 17, p. 2046–2054, June 2012.
- [11] E. L. J. U. Dung T Le, "Evaluation of Ipilimumab in Combination With Allogeneic Pancreatic Tumor Cells Transfected With a GM-CSF Gene in Previously Treated Pancreatic Cancer," *Journal of Immunotherapy*, vol. 36, no. 7, pp. 382-389, 2013.
- [12] "National Cancer Institute," 25 August 2020. [Online]. Available: <https://www.cancer.gov/about-cancer/treatment/types/immunotherapy/t-cell-transfer-therapy#what-cancers-are-treated-with-t-cell-transfer-therapy>.
- [13] "National Cancer Istitute," 24 September 2019. [Online]. Available: <https://www.cancer.gov/about-cancer/treatment/types/immunotherapy/cancer-treatment-vaccines#which-cancers-are-treated-with-cancer-treatment-vaccines>.
- [14] C. F. S. B. Coral García Fernández, "Nanomedicine in Non-Small Cell Lung Cancer: From Conventional Treatments to Immunotherapy," *Cancers*, vol. 12, no. 1609, 2020.
- [15] C. I. N.-Y. H. J. S. Matteo Vergati, "Strategies for Cancer Vaccine Development," *Journal of Biomedicine and Biotechnology*, 2010.
- [16] E. W. Peng Zhang, "History of Polymeric Gene Delivery Systems," *Topics in Current Chemistry*, vol. 375, no. 26, 2017.
- [17] T. M. P. A. A. Nouri Nayerossadat, "Viral and nonviral delivery systems for gene delivery," *Adv Biomed Res*, vol. 1, no. 27, 2012.
- [18] M. G. R. M. Á. L. C. C. S. Cristina Fornaguera, "mRNA Delivery System for Targeting Antigen-Presenting Cells In Vivo," *Adv Healthcare Mater*, 2018.
- [19] A. K. A. I. E. A. M. E. M. R. A. Samantha L Ginn, "Gene therapy clinical trials worldwide to 2017: An update," *J Gene Med*, vol. 20, no. 5, p. e3015, 2018.
- [20] W. G. Daniel Balazs, "Liposomes for Use in Gene Delivery," *J Drug Deliv*, 2011.

- [21] N. F. G. C. F. A. C. S. B. L. A. Roger Riera, "Tracking the DNA complexation state of pBAE polyplexes in cells with super resolution microscopy," *Nanoscale*, vol. 11, pp. 17869-17877, 2019.
- [22] C. S. C. L. M. A. C. A. B. S. Fornaguera Cristina, "Development of an optimized freeze-drying protocol for OM-PBAE nucleic acid polyplexes," *International Journal of Pharmaceutics*, vol. 569, 2019.
- [23] K. W. J. W. Padmanee Sharma, "Novel cancer immunotherapy agents with survival benefit: recent successes and next steps," *Nature Reviews Cancer*, vol. 11, pp. 805-812, 2011.
- [24] E. D. I. B. Sofia Farkona, "Cancer immunotherapy: the beginning of the end of cancer?," *BMC Medicine*, vol. 14, no. 73, 2016.
- [25] R. M. J. E. Kavitha Yaddanapudi, "Cancer vaccines: Looking to the future," *Oncolmunology*, vol. 2, no. 3, 2013.
- [26] G. C. G. D. Ira Mellman, "Cancer immunotherapy comes of age," *NATURE*, vol. 480, p. 480-489, 2011.
- [27] B. Lisa, "Cancer vaccines," *BMJ*, vol. 350, no. h988, 2015.
- [28] N. M. M. K. Farhood B, "CD8+ cytotoxic T lymphocytes in cancer immunotherapy: A review," *J Cell Physiol*, vol. 234, no. 6, pp. 8509-8521, 2019.
- [29] G. V. V. P. Alessandra Lopes, "Cancer DNA vaccines: current preclinical and clinical developments and future perspectives," *J Exp Clin Cancer Res*, vol. 38, no. 146, 2019.
- [30] J. B. Karolina Palucka, "Dendritic cell-based cancer therapeutic vaccines," *Immunity*, vol. 39, no. 1, pp. 38-48, 2013.
- [31] M. F. J. S. Na Shang, "Dendritic cells based immunotherapy," *Am j Cancer Res*, vol. 7, no. 10, pp. 2091-2102, 2017.
- [32] M. T. M. M. Cuicui Li, "Facilitating the presentation of antigen peptides on dendritic cells for cancer immunotherapy using a polymer-based synthetic receptor," *Medchemcomm*, vol. 8, no. 6, pp. 1207-1212, 2017.
- [33] P. d. G. R. C. Joachim Aerts, "Autologous Dendritic Cells Pulsed with Allogeneic Tumor Cell Lysate in Mesothelioma: From Mouse to Human," *Clin Cancer Res*, vol. 24, no. 4, pp. 766-776, 2017.
- [34] D. C. M. K. Jianlin Gong, "Induction of antitumor activity by immunization with fusions of dendritic and carcinoma cells," *Nature Medicine*, vol. 3, pp. 558-561, 1997.
- [35] R. F. Y. C. Rong Ni, "Synthetic Approaches for Nucleic Acid Delivery: Choosing the Right Carriers," *Life*, vol. 9, no. 59, 2019.
- [36] S. L. J. L. Katja Fiedler, "mRNA Cancer Vaccines," *Recent Results Cancer Res*, vol. 209, pp. 61-85, 2016.
- [37] "NATIONAL CANCER INSTITUTE," [Online]. Available: <https://www.cancer.gov/publications/dictionaries/cancer-drug/def/sipuleucel-t?redirect=true>.
- [38] A. P. C. W. Martin Sebastian, "Phase Ib study evaluating a self-adjuvanted mRNA cancer vaccine (RNAActive®) combined with local radiation as consolidation and maintenance treatment for patients with stage IV non-small cell lung cancer," *BMC Cancer*, vol. 14, no. 748, 2014.
- [39] K. D. L. D. A. G. F. Mark Meacham, "Physical methods for intracellular delivery: practical aspects from laboratory use to industrial-scale processing," *Journal of Laboratory Automation*, vol. 19, no. 1, pp. 1-18, 2014.
- [40] Y.-G. G. X. Y. L. Suryaji Patil, "The Development of Functional Non-Viral Vectors for Gene Delivery," *International Journal of Molecular Sciences*, vol. 20, no. 5491, 2019.
- [41] K. G. M. S. N Marasini, "Liposomes as a Vaccine Delivery System," in *Micro and Nanotechnology in Vaccine Development*, 2017, p. 221-239.

- [42] L. M. J. S. Gigante Alba, "Non-Viral Transfection Vectors: Are Hybrid Materials the Way Forward?," *Med Chem Commun*, 2019.
- [43] M. E. M. Elmatari, "Study of the encapsulation of iron nanoparticles into liposomes," 2016.
- [44] R. R. S. S. D. Abolfazl Akbarzadeh, "Liposome: classification, preparation, and applications," *Nanoscale Research Letters*, vol. 8, no. 102, 2013.
- [45] H.-J. I. Wooseung Lee, "Theranostics Based on Liposome: Looking Back and Forward," *Nuclear Medicine and Molecular Imaging*, 2019.
- [46] N. H. M. B. Sarah Engelberth, "Development of Nanoscale Approaches for Ovarian Cancer Therapeutics and Diagnostics," *Critical reviews in oncogenesis*, vol. 19, pp. 281-315, 2014.
- [47] C. H. W. G Y Wu, "Receptor-mediated in vitro gene transformation by a soluble DNA carrier system," *J Biol Chem*, vol. 262, no. 10, pp. 4429-4432, 1987.
- [48] J. K. T. K. Thomas Merdan, "Prospects for cationic polymers in gene and oligonucleotide therapy against cancer," *Adv Drug Deliv Rev*, vol. 54, pp. 715-58, 2002.
- [49] C. W. Z. R. Isabelle Degors, "Carriers Break Barriers in Drug Delivery: Endocytosis and Endosomal Escape of Gene Delivery Vectors," *Accounts of Chemical Research*, vol. 52, no. 7, pp. 1750-1760, 2019.
- [50] Y. L. D. K. L. S. Yong Liu, "Poly( $\beta$ -Amino Esters): Synthesis, Formulations, and Their Biomedical Applications," *Adv. Healthcare Mater*, vol. 8, 2019.
- [51] V. R. S. B. Pere Dosta, "Stable and efficient generation of poly( $\beta$ -amino ester)s for RNAi delivery†," *Mol. Syst. Des. Eng.*, 2018.
- [52] C. F. P. B.-V. M. G.-R. Ó. M.-C. G. M. N. R. J. B. J. S. A. C. S. B. Laura Balcells, "SPIONs' Enhancer Effect on Cell Transfection: An Unexpected Advantage for an Improved Gene Delivery System," *ACS Omega*, vol. 4, pp. 2728-2740, 2019.
- [53] P. D. A. C. V. R. S. B. Nathaly Segovia, "Oligopeptide-terminated poly( $\beta$ -amino ester)s for highly efficient gene delivery and intracellular localization," *Acta Biomaterialia*, vol. 10, pp. 2147-2158, 2014.
- [54] M. P. N. O. V. R. S. B. N. A. Nathaly Segovia, "Hydrogel Doped with Nanoparticles for Local Sustained Release of siRNA in Breast Cancer," *Adv. Healthcare Mater*, 2014.
- [55] S. S. B. W. Morteza Mahmoudi, "Superparamagnetic iron oxide nanoparticles (SPIONs): Development, surface modification and applications in chemotherapy," *Advanced Drug Delivery Reviews*, vol. 63, p. 24-46, 2011.
- [56] M. H. S. P. Samer Bayda, "Inorganic Nanoparticles for Cancer Therapy: A Transition from Lab to Clinic," *Current Medicinal Chemistry*, vol. 25, no. 34, 2018.
- [57] R. K. R. B. P. M. Sanjib Bhattacharyya, "Inorganic Nanoparticles in Cancer Therapy," *Pharm Res*, vol. 28, p. 237-259, 2011.
- [58] L. V. V. C. D. K. Nguyen Ngoc Long, "Synthesis and optical properties of colloidal gold nanoparticles," *Journal of Physics: Conference Series*, vol. 187, 2009.
- [59] M. K. M. H. B. Narges Elahi, "Recent biomedical applications of gold nanoparticles: A review," *Talanta*, vol. 184, pp. 537-556, 2018.
- [60] J. L. A. P. K. M. R. I. C. A. C. K. F. D. W. Cory Hanley, "Preferential killing of cancer cells and activated human T cells using ZnO nanoparticles," *Nanotechnology*, vol. 19, no. 29, 2008.
- [61] J. Z. J. G. Wenhua Song, "ole of the dissolved zinc ion and reactive oxygen species in cytotoxicity of ZnO nanoparticles," *Toxicol Lett*, vol. 199, no. 3, pp. 389-97, 2010.
- [62] M. C. V. C. B Dumontel, "Enhanced biostability and cellular uptake of zinc oxide nanocrystals shielded with a phospholipid bilayer," *J. Mater. Chem. B*, vol. 5, 2017.
- [63] H. E. A. S. Valentina Cauda, "Colchicine-Loaded Lipid Bilayer-Coated 50 nm

- Mesoporous Nanoparticles Efficiently Induce Microtubule Depolymerization upon Cell Uptake,” *Nano Lett*, vol. 10, p. 2484–2492, 2010.
- [64] H. Z. G. B. Sheng Tong, “Magnetic Iron Oxide Nanoparticles for Disease Detection and Therapy,” *Mater Today (Kidlington)*, vol. 31, pp. 86-99, 2019.
- [65] L. R. Gensini, “Tailoring Iron Oxide Nanoparticles for Efficient Cellular Internalization and Endosomal Escape,” *Nanomaterials*, vol. 10, no. 1816, 2020.
- [66] O. T. B. M. G. K. He Wei, “Exceedingly small iron oxide nanoparticles as positive MRI contrast agents,” *Proceedings of the National Academy of Sciences*, vol. 114, no. 9, pp. 2325-2330, 2017.
- [67] V. K. L. Rajendrakumar Santhosh Kalash, “Theranostics,” in *Biomaterials Nanoarchitectonics*, Elsevier, 2016, pp. 197-215.
- [68] J. J. P. G. Avnesh Thakor, “Clinically Approved Nanoparticle Imaging Agents,” *J Nucl Med*, vol. 57, no. 12, p. 1833–1837, 2016.
- [69] S. S. B. W. Morteza Mahmoudi, “Superparamagnetic iron oxide nanoparticles (SPIONs): Development, surface modification and applications in chemotherapy,” *Advanced Drug Delivery Reviews*, vol. 63, no. 1-1, pp. 24-46, 2011.
- [70] D. K. K. A. E. H. Meng Meng Lin, “Development of superparamagnetic iron oxide nanoparticles (SPIONS) for translation to clinical applications,” *IEEE Trans Nanobioscience*, vol. 7, no. 4, pp. 298-305, 2008.
- [71] K. R. J. I. Daniel Bobo, “Nanoparticle-Based Medicines: A Review of FDA-Approved Materials and Clinical Trials to Date,” *Pharm Res*, vol. 33, p. 2373–2387, 2016.
- [72] A. J. Burghard Thiesen, “Clinical applications of magnetic nanoparticles for hyperthermia,” *Int. J. Hyperthermia*, vol. 24, no. 6, p. 467–474, 2008.
- [73] T. R. Sneha Kelkar, “Theranostics: Combining Imaging and Therapy,” *Bioconjugate Chem.*, vol. 22, no. 10, p. 1879–1903, 2011.
- [74] S. L. X. C. Jin Xie, “Nanoparticle-based theranostic agents,” *Advanced Drug Delivery Reviews*, vol. 62, pp. 1064-1079, 2010.
- [75] S. a. W. H. Twan Lammers, “Theranostic Nanomedicine,” *Accounts of chemical research*, vol. 44, no. 10, p. 1029–1038, 2011.
- [76] F. D. V. P. N Schleich, “Iron oxide-loaded nanotheranostics: Major obstacles to in vivo studies and clinical translation,” *Journal of Controlled Release*, 2014.
- [77] A. A. Z. Y. D. Casey McQuade, “A Multifunctional Nanoplatfor for Imaging, Radiotherapy, and the Prediction of Therapeutic Response,” *Small*, 2014.
- [78] M. P. D. J. R. Andreas Hohner, “Controlled solvent-exchange deposition of phospholipid membranes onto solid surfaces,” *Biointerphases*, vol. 5, no. 1, 2010.
- [79] P. C. S. J. H. John Turkevich, “A study of the nucleation and growth processes in the synthesis of colloidal gold,” *Discuss. Faraday Soc*, vol. 11, pp. 55-75, 1951.
- [80] R. T. A. E. Christopher Ward, “Seed-Mediated Growth of Gold Nanorods: Limits of Length to Diameter Ratio Control,” *Journal of Nanomaterials*, vol. 2014, 2014.
- [81] K. E. G. K. Mats Almgren, “Cryo transmission electron microscopy of liposomes and related structures,” *Colloids and Surfaces A: Physicochemical and Engineering Aspects*, vol. 174, no. 1-2, pp. 3-21, 2000.
- [82] J. Senior, “Is half-life of circulating liposomes determined by changes in their permeability?,” *FEBS Lett*, vol. 145, no. 1, p. 109–14, 1982.
- [83] H. D. C. C. Chen Chengjun, “An overview of liposome lyophilization and its future potential,” *Journal of controlled release*, vol. 142, no. 3, pp. 299-311, 2010.
- [84] K. S. L. Prashant Jain, “Calculated Absorption and Scattering Properties of Gold Nanoparticles of Different Size, Shape, and Composition: Applications in Biological Imaging and Biomedicine,” *J. Phys. Chem.*, vol. 110, no. 14, p. 7238–7248, 2006.

- [85] P. D. A. C. V. R. S. B. Nathaly Segovia, "Oligopeptide-terminated poly( $\beta$ -amino ester)s for highly efficient gene delivery and intracellular localization," *cta Biomater*, vol. 10, no. 5, pp. 2147-2158, 2014.
- [86] V. R. S. B. Pere Dosta, "Stable and efficient generation of poly( $\beta$ -amino ester)s for RNAi delivery," *Mol. Syst. Des. Eng.*, vol. 3, pp. 677-689, 2018.
- [87] A. C. F. Monique Lapinski, "Comparison of Liposomes Formed by Sonication and Extrusion: Rotational and Translational Diffusion of an Embedded Chromophore," *Langmuir*, vol. 23, no. 23, pp. 11677-11683, 2007.
- [88] I.-I. L. D. M. Peter Njoki, "Size Correlation of Optical and Spectroscopic Properties for Gold Nanoparticles," *J. Phys. Chem. C*, vol. 111, no. 40, pp. 14664-14669, 2007.